Published in final edited form as:
Nature. 2019 October ; 574(7777): 268–272. doi:10.1038/s41586-019-1607-3.

Inducing and exploiting vulnerabilities for the treatment of liver cancer

Cun Wang[#1,2], **Serena Vegna**[#3], **Haojie Jin**[#1,2], **Bente Benedict**[#3], **Cor Lieftink**[2], **Christel Ramirez**[3], **Rodrigo Leite de Oliveira**[2], **Ben Morris**[2], **Jules Gadiot**[3], **Wei Wang**[4], **Aimée du Chatinier**[2], **Liqin Wang**[2], **Dongmei Gao**[5], **Bastiaan Evers**[2], **Guangzhi Jin**[6], **Zheng Xue**[2], **Arnout Schepers**[2], **Fleur Jochems**[2], **Antonio Mulero Sanchez**[2], **Sara Mainardi**[2], **Hein te Riele**[3], **Roderick L. Beijersbergen**[2], **Wenxin Qin**[1,#], **Leila Akkari**[3,#], **René Bernards**[2,#]

[1]State Key Laboratory of Oncogenes and Related Genes, Shanghai Cancer Institute, Renji Hospital, Shanghai Jiao Tong University School of Medicine, Shanghai, China [2]Division of Molecular Carcinogenesis, Oncode Institute. The Netherlands Cancer Institute, Plesmanlaan 121, 1066 CX Amsterdam, The Netherlands [3]Division of Tumour Biology and Immunology, The Netherlands Cancer Institute, Plesmanlaan 121, 1066 CX Amsterdam, The Netherlands [4]Division of Cell Biology, The Netherlands Cancer Institute, Plesmanlaan 121, 1066 CX Amsterdam, The Netherlands [5]Liver Cancer Institute, Zhongshan Hospital, Fudan University, Key Laboratory of Carcinogenesis and Cancer Invasion, Ministry of Education, Shanghai, China [6]Department of Pathology, Eastern Hepatobiliary Surgery Hospital, Second Military Medical University, Shanghai, China

[#] These authors contributed equally to this work.

Abstract

Liver cancer remains difficult to treat due to a paucity of drugs that target critical dependencies[1,2] and broad spectrum kinase inhibitors like sorafenib provide only modest benefit to hepatocellular carcinoma (HCC) patients[3]. Induction of senescence may represent a promising strategy for the treatment of cancer, especially when such pro-senescence therapy is combined with a second drug

Correspondence to René Bernards, Leila Akkari, and Wenxin Qin, René Bernards: Tel: +31 20 512 6973. r.bernards@nki.nl; Leila Akkari: Tel: + 31 20 512 7479. l.akkari@nki.nl; Wenxin Qin: Tel: +86 21 64436581. wxqin@sjtu.edu.cn.

Data Availability. Raw and processed data from the next-generation RNA sequencing of samples have been deposited to the NCBI Gene Expression Omnibus (GEO) under accession number GSE121276 and GSE121277. All other data can be found in the Source Data, Supplementary Information or available upon reasonable request.

Authors' Contributions: C.W. and R.B. conceived the idea and designed the study. R.B., L.A., W.Q., and R.L.B., supervised all research. R.B., L.A., C.W. and S.V. wrote the manuscript and prepared the figures. C.W. designed, performed and analysed *in vitro* experiments and interpreted the results of the xenografts model. S.V. designed, performed and analysed *in vivo* data conducted on the immunocompetent mouse models with the technical support from J.G.. H.J. and D.G. performed xenografts experiments. B.B. designed, performed and analysed neutral comet assays. C.L. and B.E. performed data analysis. C.R. performed quantitation analyses of *in vivo* staining. B.M. performed GPCR compound screen. W.W. performed immunofluorescence. A.d.C. and A.M.S. performed and analysed SHP2 experiments. G.J. provided clinical samples. R.L.d.O., L.W., Z.X., A.S., F.J., S.M. and H.t.R. provided advice for the project. All authors commented on the manuscript.

Conflicts of interest: C. Wang and R. Bernards are listed as inventors of a patent application using the "one-two punch" therapy (CDC7 inhibitor and mTOR inhibitor) for *TP53* mutant liver cancers. R. Bernards is the founder of the company "Oncosence" that exploits pro-senescence therapies for cancer.

Europe PMC Funders Author Manuscripts

Europe PMC Funders Author Manuscripts

that selectively eliminates senescent cancer cells (senolysis)[4,5]. Through a kinome-focused genetic screen, we report here that pharmacological inhibition of the DNA replication kinase CDC7 induces senescence selectively in *TP53* mutant liver cancer cells. A follow-up chemical screen identified the anti-depressant sertraline as an agent that kills HCC cells rendered senescent by CDC7 inhibition. Sertraline supressed mTOR signalling, and selective drugs targeting this pathway were highly effective in causing apoptotic cell death of CDC7 inhibitor-treated HCC cells. Mechanistically, we report that the feedback re-activation of mTOR signalling following its inhibition[6] is blocked in CDC7-inhibitor treated cells, leading to sustained mTOR inhibition and cell death. Using multiple *in vivo* liver cancer models, we show that combination of CDC7 and mTOR inhibitors results in dramatic tumour growth inhibition. More generally, our data indicate that exploiting an induced vulnerability could be an effective treatment of liver cancer.

The increase in hepatocellular carcinoma (HCC) incidence[2], the undruggable nature of HCC mutations and unresponsiveness of these tumours to therapy highlight the urgency to develop novel therapeutic approaches for this disease[7]. We and others have proposed a “one-two punch” approach to cancer therapy in which the first drug induces a vulnerability exploited by the second drug[4,5]. Senescent cells have distinct cellular features, which can confer sensitivity to senolytic agents[8,9]. Here we experimentally validate the “one-two punch” therapy for *TP53* mutant liver cancers.

To identify genes whose inactivation can induce senescence in liver cancer cells, we employed a CRISPR-Cas9 genetic screen using a lentiviral gRNA library representing all human kinases in Hep3B and Huh7 liver cancer cells[10] (Fig. 1a). We identified 38 kinases required for proliferation (Fig. 1b, Extended Data Fig. 1a, Supplementary Table 1), 14 of which could be inhibited by small molecule compounds (Fig. 1b). We screened compounds targeting these 14 kinases for their ability to induce senescence selectively in liver cancer cells (Fig. 1c). XL413, a potent inhibitor of the DNA replication kinase CDC7[11], was most selective in inducing senescence-associated β-galactosidase (SA-β-Gal, a marker of senescence) in Hep3B and Huh7 as compared to non-transformed BJ and RPE-1 human cell lines (Fig. 1c). These findings suggest that CDC7 inhibition could represent a novel senescence-inducing strategy in liver cancer.

As seen in several tumour types[12], liver cancer cell lines express higher levels of CDC7 compared to non-transformed cells (Extended Data Fig. 1b). *CDC7* expression is upregulated in tumour tissues relative to paired non-tumour tissues in two liver cancer cohorts (n=213 and n=50) (Fig. 1d) and this was confirmed at the protein level (Extended Data Fig. 1c). Moreover, in a cohort of 365 HCC patients[13] the highest tumour levels of CDC7 mRNA exhibited worst survival (Extended Data Fig. 1d).

We treated a panel of non-transformed cells and liver cancer cell lines with increasing concentrations of XL413. Interestingly, proliferation was impaired in *TP53* mutated liver cancer cell lines, while *TP53* wild-type liver cancer cell lines (SK-Hep1 and Huh6 cells) and all four non-transformed cell lines displayed no sensitivity to XL413 (Fig. 2a). The XL413-sensitive cell line HepG2 is an outlier in this respect, but carries an *ATM* mutation, which acts upstream of p53 in the DNA damage response. Importantly, shRNA-mediated *TP53*-knockdown in wild-type cells sensitized them to CDC7 inhibition (Extended Data Fig. 1e-g),

indicating a causal relationship between *TP53* mutation status and sensitivity to CDC7 inhibition.

The anti-proliferative effect of XL413 was associated with induction of senescence markers in *TP53* mutant liver cancer cells, but not in *TP53* wild-type liver cancer and non-transformed cells (Fig. 2b, Extended Data Fig. 2a) and a senescence signature[14] was enriched in XL413-treated *TP53* mutant HCC cells (Fig. 2c). The notion that CDC7 inhibition induces a senescence-like state in *TP53* mutant liver cancer cells is further supported by the finding that i) XL413 drug withdrawal does not lead to re-entry into the cell cycle in the majority of HCC cells, ii) XL413 induced senescence associated heterochromatin foci (SAHFs) and iii) XL413 induced expression of a number of cytokines, part of the Senescence Associated Secretory Phenotype[15] (SASP, Extended Data Fig. 2b-d). There was no evidence for significant apoptosis induction in XL413-treated *TP53* mutant HCC cells (Extended data Fig. 2e). Comparable results were obtained with two unrelated CDC7 inhibitors, LY3177833 and TAK-931 (Extended Data Fig. 3a-f). Consistent with this, *CDC7* gene knockdown impaired proliferation and induced senescence in *TP53* mutant liver cancer cells, but had no effect on *TP53* wild-type cells (Extended Data Fig. 3g-i).

Phosphorylation of MCM2, a target of CDC7[12], was equally suppressed by three CDC7 inhibitors in both *TP53* mutant and wild-type cells (Fig. 2d, Extended Data Fig. 4a, b), indicating no correlation between cell fate induced by CDC7 inhibitors and the degree of inhibition of its downstream targets. To further address why CDC7 inhibition selectively induces senescence in the context of mutated *TP53*, we assessed DNA damage-associated protein expression following XL413 treatment. Induction of γH2AX and DNA double strand breaks (DSB) was striking in *TP53*-mutant liver cancer cells after CDC7 inhibition compared to *TP53* wild-type cells, which instead displayed a clear upregulation of $p21^{cip1}$ (Fig. 2d, e, Extended Data Fig. 4a-c). This differential effect is most readily explained by the finding that multiple DNA repair gene signatures are upregulated in *TP53* wild-type cells (SK-Hep1 and BJ) treated with XL413, but suppressed in *TP53* mutant cells upon CDC7 inhibition (Fig. 2f, Extended data Fig. 4d, e). Consistently, inhibition of DNA repair with the ATR inhibitor AZD6738 or with the CHK1 inhibitor MK-8776 in *TP53* wild-type liver cancer cells resulted in increased DSBs when combined with XL413 treatment (Extended data Fig. 4f). CDC7 inhibition also resulted in a significant increase in duration of mitosis (Extended data Fig. 4g, h). We further confirmed the specificity of Cdc7 inhibition effects in $Trp53^{-/-}$ murine liver cancer cell lines[16] (Extended Data Fig. 4i, j). Moreover, XL413 induced senescence in *TP53* mutant, but not *TP53* wild-type non-small cell lung cancer cells (Extended data Fig. 5a, b). Similarly, in isogenic $TP53^{-/-}$ and $TP53^{+/+}$ HCT116 colon cancer cells, CDC7 inhibition only induced senescence in $TP53^{-/-}$ cells (Extended data Fig. 5c-e).

Senescence induction represents a double-edged sword for tumour control[15,17] and the potentially harmful properties of senescent tumour cells make their elimination therapeutically relevant. The high concentration of the senolytic BH3 mimetic ABT263[8] required to promote XL413-induced senescent cells apoptosis and the lack of sensitivity of these cells to dasatinib[9] prevent their translational use in the clinic (data not shown). We therefore sought to identify less toxic compounds to selectively kill senescent liver cancer

cells using a G Protein Coupled Receptor compound library screen in both proliferating and XL413-treated senescent Huh7 cells (Extended data Fig. 6a). Only the anti-depressant sertraline exhibited differential effects on proliferating versus XL413-induced senescent cells (Extended data Fig. 6b, c), as it had modest effects on proliferating cells, but induced significant apoptosis post XL413 treatment (Extended data Fig. 6d-f).

The concentration of sertraline needed to induce senescent-cell apoptosis precludes its clinical use. We therefore explored the mechanism through which sertraline selectively induces apoptosis in XL413-induced senescent cells. We analysed different signalling pathways in sertraline treated cells and found that sertraline treatment leads to inhibition of p-S6RP and p-4EBP1 in XL413-induced senescent cells (Extended data Fig. 6g) suggesting that the apoptotic effects of sertraline may involve regulation of mTOR signalling, as previously reported[18]. Consistently, GSEA analyses following RNA-sequencing of XL413 and sertraline sequential treatment indicated enrichment of a gene set related to downregulation of mTOR signalling (Extended data Fig. 6h).

To explore whether mTOR inhibitors may be used as effective drugs in our XL413-induced senescence models, we analysed the activity of two mTOR inhibitors (AZD8055 and AZD2014). Both inhibitors induced apoptosis in XL413-treated *TP53* mutant liver and lung cancer cells, while only limiting proliferation of untreated cells (Fig. 3a, b, Extended Data Fig. 6i-k). As expected, sequential treatment with AZD8055 did not lead to apoptosis in non-senescent, XL413-pretreated *TP53* wild-type liver cancer cells (Extended Data Fig. 6l). Importantly, mTOR signalling was further inhibited in XL413-induced senescent cells exposed to AZD8055 or AZD2014 compared to proliferating cells (Fig. 3c, Extended Data Fig. 6m).

mTOR blockade results in a feedback loop reactivation of mTOR signalling through Receptor Tyrosine Kinase (RTK) engagement, thus limiting mTOR inhibitor efficacy[6]. We explored the feedback activation of mTOR signalling in time-course experiments and found that rapid re-activation of mTOR, as judged by multiple site phosphorylation of S6RP and 4EBP1, was observed in proliferating Hep3B cells, but not in senescent Hep3B cells (Fig. 3d). This feedback re-activation loop may stem from both transcriptional and biochemical activation of EGFR, PDGFRβ and IGF-1R, leading to increase p-SHP2, a process that is disrupted in XL413-treated Hep3B cells (Extended Data Fig. 7a-c). Combining mTOR and SHP2 inhibitors resulted in inhibition of feedback reactivation of mTOR signalling and caused cell death in proliferating Hep3B cells (Fig. 3e-g), indicating that suppression of mTOR reactivation is critical for apoptosis induction in senescent cells. Supporting these findings, mTOR inhibition also induced AKT activation in proliferating cells and AKT inhibition synergized with mTOR blockade to induce cell death (Extended Data Fig. 7d-f). Oncogene-induced senescent primary fibroblasts were insensitive to AZD8055 (Extended data Fig. 8a, b), indicating that not all senescent cells are killed by mTOR inhibition. Importantly, feedback re-activation of mTOR was not impaired in cisplatin or alisertib-induced Hep3B senescent cells and consequently, no cell death was observed following mTOR inhibition (Extended data Fig. 8c-e). These data indicate that mTOR inhibitor efficacy has context dependency and relies on CDC7-inhibitor treatment.

To assess whether our *in vitro* findings can be recapitulated *in vivo*, we generated Huh7 and MHCC97H xenografts. XL413-treated tumours showed increased DNA damage and SA-β-gal^{+} senescent cells as compared to vehicle, AZD8055 or combination-treated tumours, indicating that CDC7 inhibition induces senescence *in vivo* (Extended Data Fig. 9a). No SA-β-gal staining was observed in *TP53* wild-type SK-Hep1 tumours treated with XL413, consistent with the notion that CDC7 inhibition only induces senescence in a *TP53* mutant background (Extended data Fig. 9b). Compared to sorafenib treatment, the combination of XL413 and AZD8055 elicited a more effective growth inhibition, and combination-treated *TP53*-mutant xenografts displayed diminished proliferation and p-4EBP1 activation associated with increased apoptosis (Fig. 4a, Extended data Fig. 9c-g).

In immune-competent, somatic murine models of HCC[19] (Extended Data Fig. 10a), treatment with XL413 induced senescence specifically in *Trp53* deficient tumours (*Myc*^{OE};*Trp53*^{KO}), but not in *Myc*^{OE};*Pten*^{KO} tumours (Extended Data Fig. 10b). *Myc*^{OE};*Trp53*^{KO} tumour-bearing mice receiving XL413 or AZD8055 monotherapy showed a modest reduction in tumour volume and increased animal lifespan, while XL413 combined with AZD8055 was well-tolerated, significantly reduced tumour burden and increased survival compared to either monotherapy or to sorafenib in this aggressive HCC model (Fig. 4b-e, Extended Data Fig. 10c-f). Importantly, the number of SA-β-gal and p16^{INK4A} positive cells was decreased in the combination-treated group, suggesting that senescent cells were efficiently eliminated by AZD8055 treatment (Fig. 4f, g, Extended Data Fig. 10g, h). An influx of macrophages (CD11b^{+}Ly6C^{-}Ly6G^{-}), CD4^{+} T cells and increased proliferation of CD4^{+} and CD8^{+} T cells were observed post-XL413 at the intermediate time-point of treatment. These changes were largely lost in the combination-treated groups and in XL413-treated endpoint tumours (Extended Data Fig. 10i). Withdrawal of XL413 after induction of senescence *in vivo* did not alter the absolute number of senescent cells, suggesting that infiltrating immune cells were unable to efficiently clear senescent cells (Extended Data Fig. 10j).

Our data indicate that CDC7 inhibitor pro-senescence therapy combined with mTOR inhibitor may deliver clinical benefit in liver cancer, by alleviating both cell-autonomous[20] and non-autonomous[21] attributes of senescent cells, thus reducing risk of tumour relapse. Immune surveillance, while mobilized, had limited effect post-CDC7 inhibition. It will be worthwhile to investigate whether combining immunotherapy, which has demonstrated activity in HCC[22], with pro-senescence therapy can activate the cytotoxic potential of recruited immune cells in tumours treated with pro-senescence therapy.

Methods

Cell lines

The human liver cancer cell lines, Hep3B, Huh7, HepG2, SNU182, SNU398, SNU449, Huh6, SK-Hep1 and PLC/PRF/5 were provided by Erasmus University (Rotterdam, Netherlands). MHCC97H and HCCLM3 were provided by the Liver Cancer Institute of Zhongshan Hospital (Shanghai, China). The majority of liver cancer cell lines were established from hepatocellular carcinoma (HCC). Among them, SK-Hep1 was established from an endothelial tumour in the liver and Huh6 is a hepatoblastoma cell line. Liver cancer

cells were cultured in DMEM with 10% FBS, glutamine and penicillin/streptomycin (Gibco®) at 37 °C / 5% CO_2. The liver cancer cell lines were authenticated by applying short tandem-repeat (STR) DNA profiling. HCT116 (*TP53*$^{+/+}$ and *TP53*$^{-/-}$) cells were provided by Dr. Bert Vogelstein. hTERT immortalized BJ fibroblasts and retinal pigment epithelial cells (RPE-1) were provided by Xiaohang Qiao (Netherlands Cancer Institute, Amsterdam, The Netherlands). TIG-3 immortalized with hTERT and MCF-10A cells were provided by Li Li (Netherlands Cancer Institute, Amsterdam, The Netherlands). Two mouse liver cancer cell lines with different genetic background (*Nras*^{G12V};*Myc*^{OE};*Trp53*$^{-/-}$ and *Nras*^{G12V};*Myc*^{OE};*Cdkn2a*$^{ARF-/-}$) were provided by Lars Zender (University Hospital Tubingen, Tuebingen, Germany). Mycoplasma contamination was excluded via a PCR-based method.

Compounds and antibodies

XL413 (S7547), BMS265246 (S2014), ON-01910 (S1362), PD0166285 (S8148), LDC000067 (S7461), PF-03814735 (S2725), D 4476 (S7642), VE-821 (S8007), AZD8055 (S1555), AZD2014 (S2783), AZD6738 (S7693) and MK-8776 (2735) were purchased from Selleck Chemicals. THZ531 (A8736) was purchased from ApexBio. XL413 (205768), BLU9931 (206192) and LY3177833 (206762) were purchased from MedKoo. TAK-931 (CT-TAK931) was purchased from Chemietek. XL413 (A13677) was also purchased from AdooQ BIOSCIENCE. The SHP2 inhibitor used in this study is covered by a patent application (WO 2015/107495A1; compound #57) and was synthesized as described previously[23].

Antibodies against HSP90 (sc-7947, sc-13119), p53 (sc-126), p21 (sc-6246), and SHP2 (sc-280) were purchased from Santa Cruz Biotechnology. Antibodies against CDC7 (ab77668), p-MCM2 (ab109133, ab133243), MCM2 (ab4461), p-SHP2 (ab62322), PCNA (ab2426), and Cleaved caspase-3 (ab2303) were purchased from Abcam. Antibodies against γH2AX (#9718), p-S6RP (#4856, #5364), S6RP (#2317), p-4EBP1 (#9456, #2855, #9455), 4EBP1 (#9644), p-IGF-1R/INSR (#3024), IGF-1R (#9750), p-PDGFRβ (#3161), PDGFRβ (#4564), p-AKT (#4060), and AKT (#2920) were purchased from Cell Signalling. EGFR antibody (610017) was purchased from BD Biosciences. H3K9Me3 antibody (49-1008) and p-EGFR (44-788) were from Thermo Fisher Scientific.

Pooled ‘stress lethal’ CRISPR screen

For the design of the kinome CRISPR library, 5,971 gRNAs targeting 504 human kinases, 10 essential genes and 50 non-targeting gRNAs were selected. Oligos with gRNA sequences flanked by adapters were ordered from CustomArray Inc (Bothell, WA) and cloned as a pool by GIBSON assembly in LentiCRISPRv2.1. The kinome CRISPR library was introduced to Hep3B and Huh7 cells by lentiviral transduction. Cells stably expressing gRNA were cultured for 14 days. The abundance of each gRNA in the pooled samples was determined by Illumina deep sequencing. gRNAs prioritized for further analysis were selected by the fold depletion of abundance in T14 sample compared with that in T0 sample, using methods as described previously[24].

Compound screens

A Induction of senescence screen: We performed a compound screen including 10 small-molecule inhibitors that targeting the 14 hits identified in the CRISPR screen. Compounds used for this screen are described in Fig. 1c. Each compound was evaluated in two liver cancer cell lines (Hep3B and Huh7) and two non-transformed cell lines (BJ and RPE-1) using 5 different concentrations. The screens were performed in three replicates of each cell line. Senescence associated-β-galactosidase (SA-β-Gal) staining was performed after 4 days of treatment.

B Killing senescent cells screen: Cells were screened for sensitivity against a panel of 260 small-molecule inhibitors from a GPCR compound library (L2200, Selleck Chemicals). Briefly, Huh7 cells were treated with 10 μM XL413 for 5 days and then control cells and XL413-treated cells were plated in 96-well plates. All compounds from GPCR library were tested at 4 different concentrations. Each plate included 8 wells containing DMSO (negative control) and 8 wells containing 10 μM PAO (positive control). Cell viability in each well was determined using the CellTiter-Blue reagent (Promega). The relative survival of control cells and XL413-treated senescent cells in the presence of drug was normalized against control conditions (untreated cells) after subtraction of background signal.

SA-β-Gal staining

SA-β-Gal staining was performed either in 6-well or 96-well plates (for *in vitro* studies), on 10-μm-thick cryosections from xenografted tumours or on 8-μm-thick cryosections from HDTVi-generated Myc^{OE};$Trp53^{KO}$ tumours, using a commercial kit (Sigma), following the manufacturer's instructions.

Protein lysate preparation and western blots

Cells were washed with PBS and lysed with RIPA buffer supplemented with Complete Protease Inhibitor (Roche) and Phosphatase Inhibitor Cocktails II and III (Sigma). Protein quantification was performed with the BCA Protein Assay Kit (Pierce). All lysates were freshly prepared and processed with Novex NuPAGE Gel Electrophoresis Systems (Thermo Fisher Scientific) followed by western blotting.

Immunohistochemical staining

HCC specimens were obtained from 80 patients (from 26-76 years old) who underwent curative surgery in Eastern Hepatobiliary Hospital of the Second Military Medical University in Shanghai, China. Patients were not subjected to any preoperative anti-cancer treatment. Ethical approval was obtained from the Eastern Hepatobiliary Hospital Research Ethics Committee, and written informed consent was obtained from each patient. Of these cases, 12 patients are female and 68 patients are male. 59 patients had an HBV infection background. Clinical information, including tumour number, diameter of tumour, tumour differentiation, serum AFP, status of cancer recurrence, disease-free survival and death from recurrence was collected. For immunohistochemical analysis, formalin-fixed paraffin-embedded samples from HCC patients were probed with CDC7 antibody (ab77668, Abcam). Formalin-fixed paraffin-embedded samples were also obtained from xenograft

tumours or tumours from immunocompetent somatic murine models and then probed with antibodies against PCNA (ab2426, Abcam), Cleaved caspase-3 (ab2303, Abcam), p-4EBP1 (#2855, Cell signalling) or p16 (ab54210, Abcam). Following incubation with the primary antibodies, positive cells were visualized using DAB+ as a chromogen. For the analysis of p16 and SA-β-Gal staining, slides were digitally processed using the Aperio ScanScope (Aperio) at a magnification of 20X. Nodule size was drawn by hand in HALO™ image analysis software (Indica Labs) and an algorithm was designed with the Multiplex IHC v1.2 module to quantify the number of positive cells[25] either as absolute or per mm^2, as indicated in figure legends.

Long-term cell proliferation assays (colony formation)

Cells were cultured and seeded into 6-well plates at a density of 0.5-4 × 10^4 cells per well, depending on growth rate, and were cultured in medium containing the indicated drugs for 10-14 days (medium was changed twice a week). Cells were fixed with 4% formaldehyde in PBS and stained with 0.1% crystal violet diluted in water.

Plasmids

All lentiviral shRNA vectors were retrieved from the arrayed TRC human genome-wide shRNA collection.

shCDC7#1:TRCN0000003168_CCGGGCCACAGCACAGTTACAAGTACTCGAGTACTTGTAACTGTGCTGTGGCTTTTT;

shCDC7#2:TRCN0000196542_CCGGGAAGCTTTGTTGCATCCATTTCTCGAGAAATGGATGCAACAAAGCTTCTTTTTTG.

shp53#1:TRCN0000010814_CCGGGAGGGATGTTTGGGAGATGTACTCGAGTACATCTCCCAAACATCCCTCTTTTT

shp53#2:TRCN0000003754_CCGGTCAGACCTATGGAAACTACTTCTCGAGAAGTAGTTTCCATAGGTCTGATTTTT

shp53#3:TRCN0000003755_CCGGGTCCAGATGAAGCTCCCAGAACTCGAGTTCTGGGAGCTTCATCTGGACTTTTT

Incucyte cell proliferation assay and apoptosis assay

Indicated cell lines were seeded into 96-well plates at a density of 1,000-8,000 cells per well, depending on growth rate and the design of the experiment. About 24 hours later, drugs were added at the indicated concentrations using the HP D300 Digital Dispenser (HP). Cells were imaged every 4 h using the Incucyte ZOOM (Essen Bioscience). Phase-contrast images were analysed to detect cell proliferation based on cell confluence. For cell apoptosis, caspase-3/7 green apoptosis assay reagent was added to culture medium and cell apoptosis was analysed based on green fluorescent staining of apoptotic cells.

RNA sequencing

RNA (one sample per cell line / condition) was isolated using Trizol, and cDNA libraries were sequenced on an Illumina HiSeq2500 to obtain 65-bp single-end sequence reads. Reads were aligned to the GRCh38 human reference genome. Gene set enrichment analysis (GSEA) was performed using gene set enrichment analysis software as described previously[26]. The FRIDMAN_SENESCENCE_UP gene set was used to assess the enrichment of senescence-associated genes in the XL413-treated versus control cells[14]. DNA damage repair-related gene sets were used to assess the enrichment of DNA damage repair-associated gene in the XL413-treated versus control cells. Enrichment scores were corrected for gene-set size (normalized enrichment score). The PENG_RAPAMYCIN_RESPONSE_DN gene set was used to assess the enrichment of downregulation of mTOR signalling in liver cancer cells sequentially treated with XL413 and sertraline versus control cells[27]. The *P* value estimates the statistical significance of the enrichment score for a single gene set as described previously[26]. The exact *P* value is shown in the figures unless the *P* value < 0.001.

Immunofluorescence and image analysis

For immunofluorescence microscopy, cells were seeded on glass coverslips and cultured in the presence of 10 μM XL413 for 7 days. Cells were fixed in 2% paraformaldehyde and permeabilized with 0.2% Triton X-100 for 5 min, blocked with PBS containing 2% bovine serum albumin (BSA; Sigma-Aldrich) for 45 min and subsequently incubated with H3K9Me3 antibody (Thermo Fisher Scientific, 49-1008) and goat anti-rabbit Alexa Fluor 488 (Invitrogen; 1:200) for 1h, respectively. Nuclei were stained with 4,6-diamidino-2-phenylindole (DAPI). Samples were mounted on glass slides in Mowiol after three washing steps with PBS. Images were acquired with a Leica TCS SP5 confocal microscope with a 63x (NA 1.4) oil objective. Image processing was performed using ImageJ software.

Neutral comet assay

To detect DNA double strand breaks (DSBs), neutral comet assays were performed as previously described[28]. Shortly, cells were harvested and embedded in 1% low-gelling-temperature agarose (Sigma-Aldrich). Cell suspension was used to make gels onto Comet assay slides (Trevigen). Cells in the agarose gels were lysed at 37 °C in lysis buffer (2% sarkosyl, 0.5M Na_2EDTA and 0.5 mg/ml Proteinase K) overnight. Subsequently, slides were washed three times for 30 minutes at room temperature in electrophoresis buffer (90 mM Tris-HCl pH=8.5, 90 mM Boric Acid and 2 mM Na_2EDTA). Electrophoresis was performed for 25 minutes at 20 V in electrophoresis buffer. Afterwards, slides were washed once with MQ and DNA was stained using 2.5 μg/ml Propidium Iodide (PI) in MQ. Individual comets were imaged with Zeiss AxioObserver Z1 inverted microscope. Tailmoments of individual comets were assessed using the CASP software. For each condition, at least 50 cells were analysed.

Time-lapse live imaging

To allow visualization of chromosomes, cells were transduced with a histone H2B-GFP (LV-GFP, Addgene plasmid#25999). Cells were then plated 24 hours before starting the

microscope acquisition. XL413 (10 μM) was added in the medium 1 hour before starting the movie. Cells were filmed over 96 hours and pictures were taken every 10 minutes. For each condition filmed, 5 different fields were selected. In each field we randomly choose and followed cells entering in mitosis (nuclear envelope breakdown, NEBD, was used as indicator of mitotic division onset).

qRT-PCR

Total RNA was extracted from cells using Trizol reagent from Invitrogen or Quick-RNA MiniPrep from Zymo Research. cDNA synthesis was performed using Maxima Universal First Strand cDNA Synthesis Kit from Thermo Scientific. qPCR reactions were performed with FastStart Universal SYBR Green Master (Rox) from Roche. The experiments were performed according to the manufacturer's instructions. The sequences of the primers used for qRT-PCR analyses were the following.

IL6_Forward, ACTCACCTCTTCAGAACGAATTG; IL6_Reverse, CCATCTTTGGAAGGTTCAGGTTG; IL8_Forward, TTTTGCCAAGGAGTGCTAAAGA; IL8_Reverse, AACCCTCTGCACCCAGTTTTC; MMP1_Forward, TTGTGGCCAGAAAACAGAAA; MMP1_Reverse, TTCGGGGAGAAGTGATGTTC; MMP3_Forward, CAATTTCATGAGCAGCAACG; MMP3_Reverse, AGGGATTAATGGAGATGCCC; CXCL1_Forward, CTTCCTCCTCCCTTCTGGTC; CXCL1_Reverse, GAAAGCTTGCCTCAATCCTG; CXCL10_Forward, GCTGATGCAGGTACAGCGT; CXCL10_Reverse, CACCATGAATCAAACTGCGA; EGFR_Forward, AGGCACGAGTAACAAGCTCAC; EGFR_Reverse, ATGAGGACATAACCAGCCACC; IGF-IR_Forward, TCGACATCCGCAACGACTATC; IGF-IR_Reverse, CCAGGGCGTAGTTGTAGAAGAG; INSR_Forward, AAAACGAGGCCCGAAGATTTC; INSR_Reverse, GAGCCCATAGACCCGGAAG; PDGFRB_Forward, AGCACCTTCGTTCTGACCTG; PDGFRB_Reverse, TATTCTCCCGTGTCTAGCCCA; GAPDH_Forward, AAGGTGAAGGTCGGAGTCAA; GAPDH_Reverse, AATGAAGGGGTCATTGATGG. All reactions were run in triplicate.

Human Phospho-RTK Array

Phospho-RTK Arrays were utilized to analyse alterations of kinase signalling in response to AZD8055 treatment in Hep3B cells according to the manufacturer's instructions (R&D systems).

Xenografts

All animals were manipulated according to protocols approved by the Shanghai Medical Experimental Animal Care Commission and Shanghai Cancer Institute. Maximum permitted tumour volumes were 2,000 mm^3. Huh7 and MHCC97H cells (5×10^6 cells per mouse) were injected subcutaneously into the right posterior flanks of 6-week-old BALB/c nude mice (male, 6-10 mice per group). Tumour volume based on calliper measurements was calculated by the modified ellipsoidal formula: tumour volume = ½ length × $width^2$. After tumour establishment, mice were randomly assigned to 6 days / week treatment with vehicle, XL413 (50-100 mg/kg, oral gavage), AZD8055 (10-20 mg/kg, oral gavage), or a drug combination in which each compound was administered at the same dose and schedule

Europe PMC Funders Author Manuscripts

as single agent. For sorafenib treatment assay, Huh7 and MHCC97H-pLKO cells (5×10^6 cells per mouse) were injected subcutaneously into the right posterior flanks of 6-week-old BALB/c nude mice (male, 6 per group). Mice were randomly assigned to treatment 6 days / week with vehicle or sorafenib (30 mg/kg, daily gavage). The investigators were not blinded to allocation during experiments and outcome assessment.

Immunocompetent HCC murine models

All animal study protocols were approved by the NKI Animal Welfare Body. Vectors for hydrodynamic tail-vein injection (HDTVi) were prepared using the EndoFree-Maxi Kit (Qiagen) and resuspended in a sterile 0.9% NaCl solution/plasmid mix containing 5 μg of pT3-c-myc (Addgene 92046), 5 μg of pX330-p53 (Addgene 59910) or pX330-Pten (Addgene 59909), and 2.5 μg of CMV-SB13 Transposase. A total volume mix corresponding to 10% of body weight was injected via lateral tail vein in 5-7 seconds into 6-8 weeks-old females C57Bl/6 mice (Janvier laboratories). Animals were monitored by weekly MRI post-HDTVi. MRI was performed in ParaVision 6.0.1 on a 7T Bruker BioSpec 70/20 USR with a ^{1}H transmit-receive volume coil. T2-weighted images were acquired under 1-2% isoflurane in air/oxygen using a respiratory-gated sequence with TR/TE = 2500/25ms, 32 x 24mm field of view (320 x 240 matrix, resolution of 0.1mm), 30 x 0.7mm axial slices and 4 averages. MRI images were analysed with MIPAV (Medical, Image, Processing, Analysis, and Visualization software) to calculate tumour volume. The investigators were not blinded to allocation during experiments and outcome assessment.

When HCC were first visible by MRI, 14-21 days post HDTVi, tumour size-matched mice were randomized over the treatment groups: vehicle, XL413, AZD8055, combination of XL413 and AZD8055, or sorafenib. Mice were dosed 6 days/week with vehicle, XL413 (100 mg/kg, oral gavage), AZD8055 (20 mg/kg, oral gavage), a drug combination in which XL413 and AZD8055 were administered at the same dose as single agent, or with sorafenib (30mg/kg, oral gavage). For time point analysis, mice were sacrificed 14-16 days post-treatment initiation, while for survival curve and endpoint analysis, the treatment continued until mice where symptomatic (tumour reached a total volume ≥ 2 cm^3).

No toxicity has been observed over the monotherapy groups. 17% of animals showed therapy-induced adverse events in the XL413 + AZD8055 treatment group while 83% of mice showed well-tolerated treatment response.

For SA-β-Gal staining quantitation, the sample size is described as following: vehicle, n=41 biologically independent nodules out of 7 mice; XL413, n=81 biologically independent nodules out of 11 mice; AZD8055, n=26 nodules out of 3 mice; combination, n=101 nodules out of 13 mice). For p16 staining quantitation, the sample size is described as following: vehicle, n=23 biologically independent nodules out of 3 mice; XL413, n=43 biologically independent nodules out of 5 mice; AZD8055, n=37 nodules out of 3 mice; combination, n=59 nodules out of 8 mice.

Flow Cytometry

Mouse livers were perfused with PBS and then dissociated into single-cell suspension using the Liver Dissociation kit (Miltenyi Biotec) and the gentleMACS™ Octo Dissociator

Europe PMC Funders Author Manuscripts

following manufacturer's instructions. The cell suspension was passed through a 100-μm cell strainer (Corning) and then centrifuged at 300g for 10 min at 4°C and washed 3 times in FACS buffer. Samples were incubated with anti-CD16/CD32 antibody (BD Biosciences) for 15 minutes and then stained with the indicated antibodies (Supplementary Table 2) following standard procedures. Samples were fixed with eBioscience fixation/ permeabilization kit (Invitrogen) and Ki67 antibody was used for intracellular staining. The signal was detected by using a 4 lasers Fortessa® flow cytometer (Becton Dickinson). Analyses were carried out using FlowJo® software. The gating strategy is provided in supplementary information. For Macrophages, CD4 and CD8 T cells, the sample size was described as following: vehicle, intermediate timepoint n=7 mice, endpoint n=8 mice; XL413, intermediate timepoint n=3 mice, endpoint n=6 mice; AZD8055, intermediate timepoint n=3 mice, endpoint n=5; combination, intermediate timepoint n=6 mice, endpoint n=7 mice. $Ki67^+$ cells in CD4 and CD8 T cell populations: vehicle, intermediate timepoint n=7 mice, endpoint n=8 mice; XL413, intermediate timepoint n=3 mice, endpoint n=4 mice; AZD8055, intermediate timepoint n=3 mice, endpoint n=5; combination, intermediate timepoint n=6 mice, enpoint n=3 mice.

Extended Data

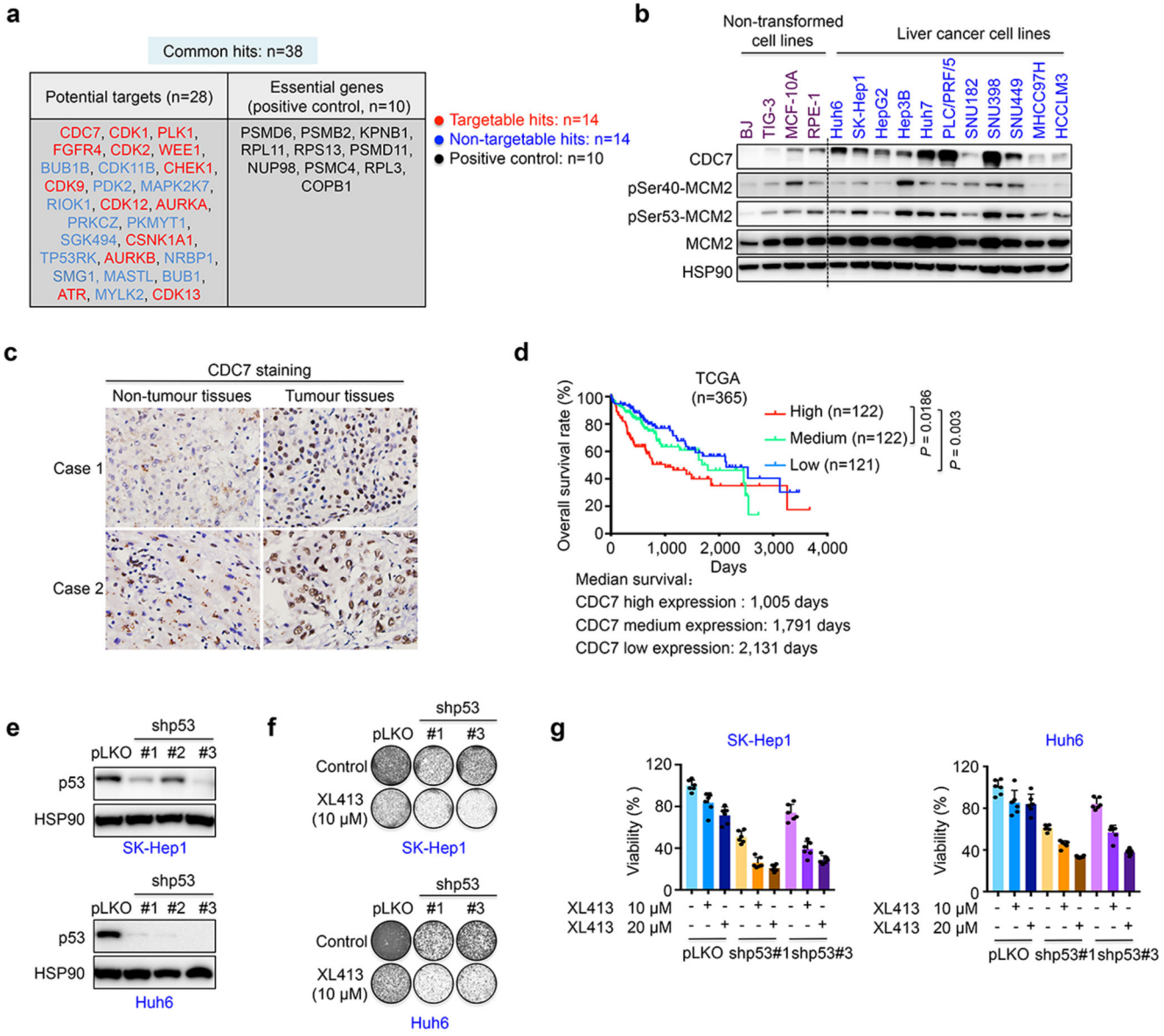

Extended Data Figure 1. Upregulation of CDC7 mRNA correlates with poor prognosis of HCC patients and *TP53* knockdown sensitizes *TP53* wild-type liver cancer cells to CDC7 inhibitor.

a, 38 common hits (among top 50 most strongly depleted hits in each cell line) were identified by CRISPR screen in Hep3B and Huh7 cells. Hits in red represent factors targetable with small molecule compounds. Blue font represents non-targetable hits. **b,** Western blot analysis of CDC7, p-MCM2 and MCM2 levels in non-transformed cell lines and liver cancer cell lines with HSP90 serving as a loading control. **c,** Immunohistochemical analysis showing increased CDC7 expression in HCC tissues compared to paired adjacent non-tumour tissues. **d,** According to the level of CDC7 mRNA obtained from the TCGA database (n=365), HCC patients were classified into 3 groups: the top 33.3% were considered as high expression, the medium 33.3% were considered as intermediate expression and the lowest 33.3% were considered as low expression. Kaplan-Meier curves

Europe PMC Funders Author Manuscripts

depicting that upregulation of CDC7 mRNA correlates with poor prognosis of HCC patients. Statistical significance was calculated using a two-sided Log-rank test. **e,** *TP53* wild-type liver cancer cell lines (SK-Hep1 and Huh6) were stably transduced with control pLKO vector or with three independent shRNAs targeting *p53* (shp5*3*#1, shp5*3*#2, shp5*3*#3). Based on knockdown efficiency, shp53#1 and shp53#3 were selected for further experiments. **f,** SK-Hep1 and Huh6 expressing a control shRNA (pLKO) or knockdown of *p53* (shp53) were exposed to the indicated concentrations of XL413 in colony formation assays. Cells were fixed, stained and photographed after 10-14 days of culture. **g,** Control or shp53 expressing SK-Hep1 and Huh6 were exposed to the indicated concentrations of XL413 for 5 days. CellTiter-Blue viability assays revealed that *TP53* knockdown synergizes with XL413 in SK-Hep1 and Huh6 cells (Graphs represent mean ± s.d. from six technical replicates). For gel source images, see Supplementary Figure 1. Data in **a-b, e-g** are representative of three independent biological experiments. Data in **c** are representative images from immunohistochemical analyses using a tissue microarray (TMA) containing 80 HCC specimens.

Europe PMC Funders Author Manuscripts

Europe PMC Funders Author Manuscripts

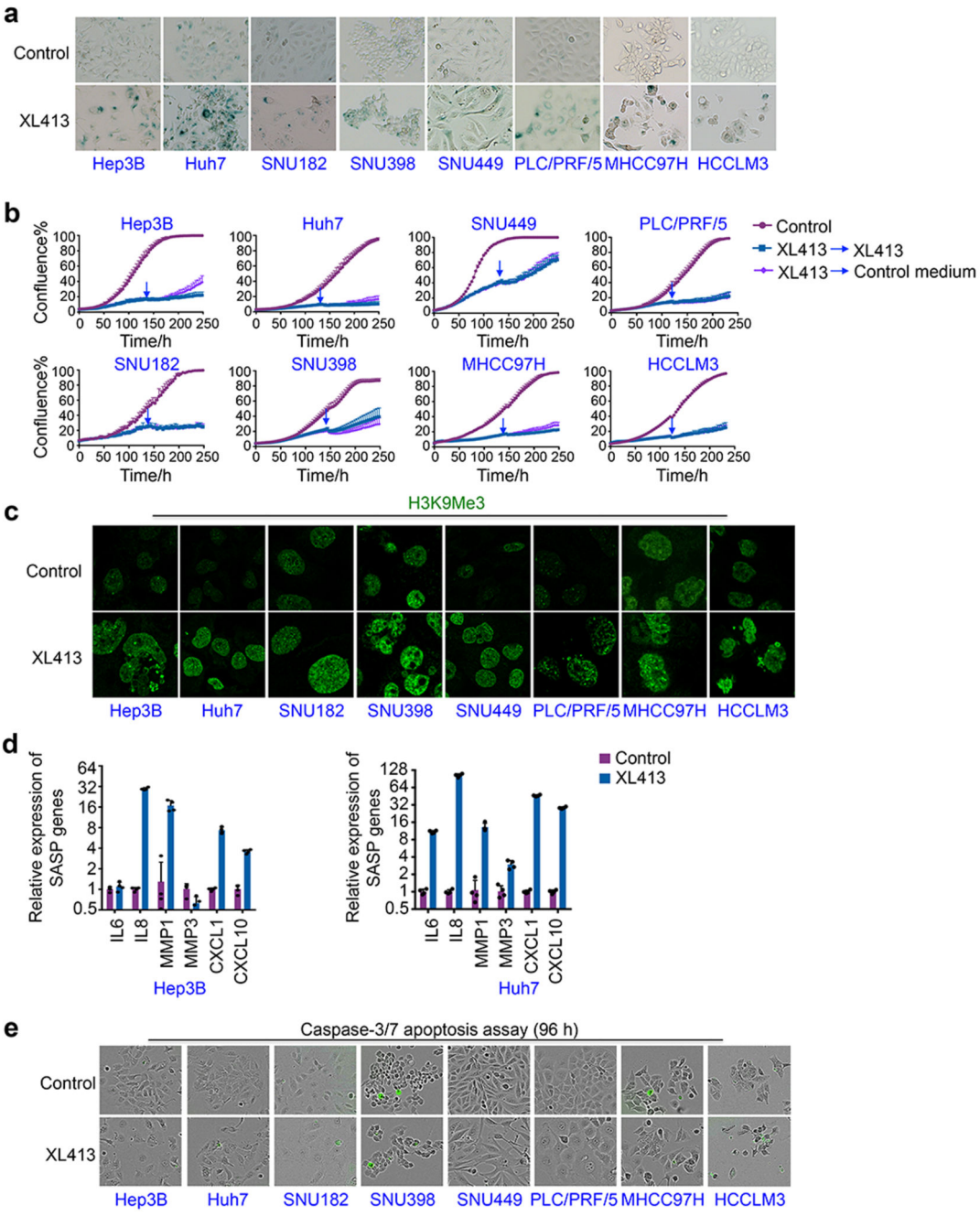

Extended Data Figure 2. CDC7 inhibition induces senescence selectively in *TP53* mutant liver cancer cells.

a, *TP53* mutant liver cancer cell lines were cultured in the presence of 10 μM XL413 for 4 days, which induces senescence as detected by SA-β-gal staining. **b,** Growth curves measured by Incucyte live cell analyses of *TP53* mutant liver cancer cell lines either untreated, continuously treated with XL413, or treated with 10 μM of XL413 for 5 or 6 days prior to treatment withdrawal (Graphs represent mean ± s.d. from five technical replicates). **c,** Representative images of H3K9Me3 staining in *TP53* mutant liver cancer cell lines

exposed to 10 μM XL413 for 7 days. **d,** XL413 treatment induces a senescence-associated secretory phenotype (SASP) in Hep3B and Huh7 cells treated with 10 μM XL413 for 7 days. mRNA expression of SASP genes was determined by qRT-PCR analysis (Graphs represent mean ± s.d. from four technical replicates). **e,** Liver cancer cells were cultured in the presence of 10 μM XL413 for 4 days and apoptotic cells were visualized by caspase-3/7 apoptosis assay. Data in **a** are representative of three independent biological experiments. Data in **b-e** are representative of two independent biological experiments.

Europe PMC Funders Author Manuscripts

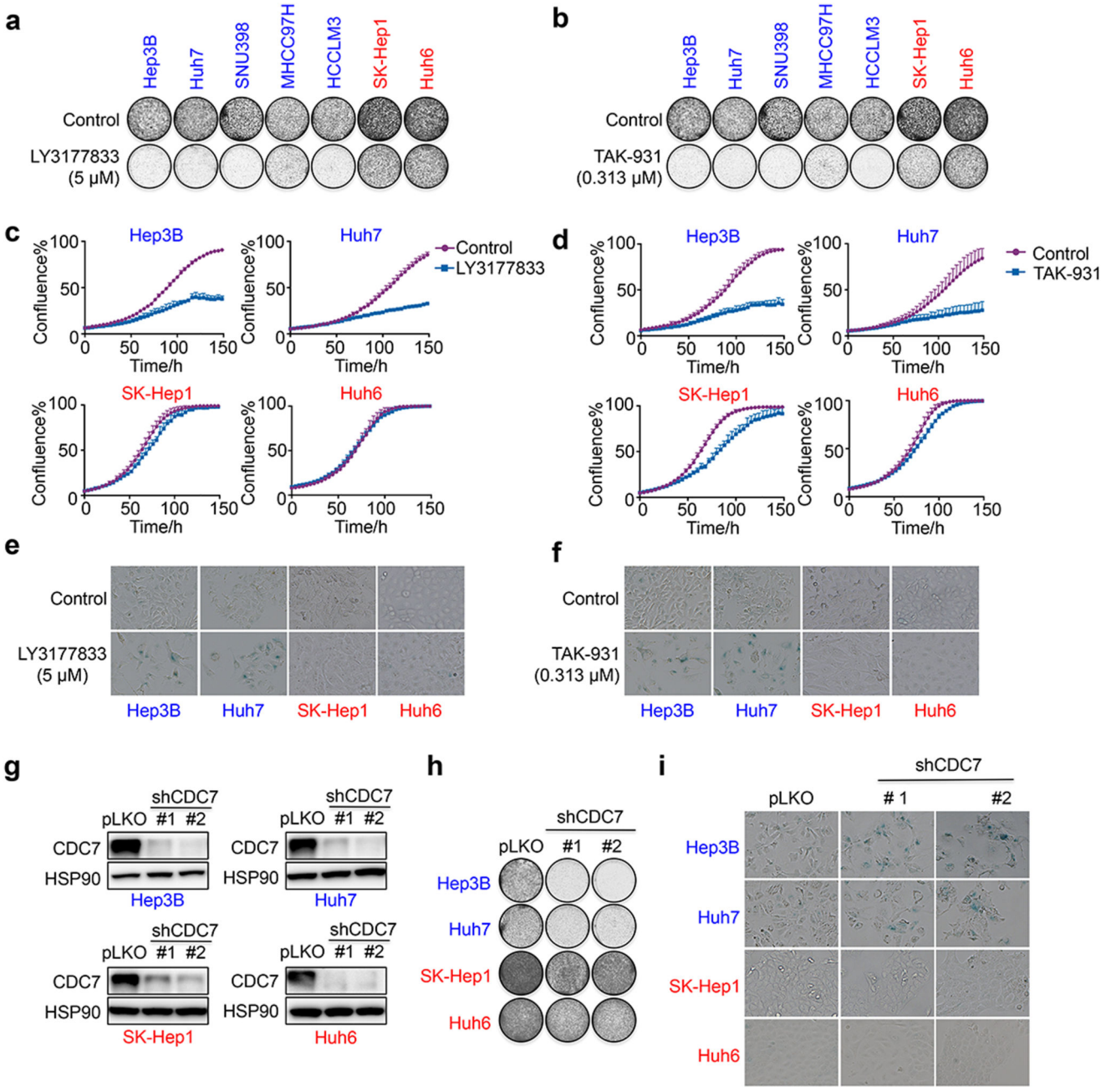

Extended Data Figure 3. Pharmacological or genetic inhibition of CDC7 induces a senescent phenotype in *TP53* mutant liver cancer cells.

a, b, *TP53* mutant liver cancer cell lines (Hep3B, Huh7, SNU398, MHCC97H and HCCLM3; blue) and *TP53* wild-type liver cancer cell lines (SK-Hep1 and Huh6; red) were seeded at low confluence and grown in the absence or presence of the CDC7 inhibitors LY3177833 or TAK-931 at the indicated concentrations, in long-term colony formation assays. Cells were fixed, stained, and photographed after 10-14 days of culture. **c, d,** Growth curves measured by Incucyte live cell analyses of *TP53* mutant liver cancer cell lines (Hep3B and Huh7; blue) and *TP53* wild-type liver cancer cell lines (SK-Hep1 and Huh6;

Europe PMC Funders Author Manuscripts

red) exposed to LY3177833 or TAK-931 (Graphs represent mean ± s.d. from four technical replicates). **e, f,** Liver cancer cells were cultured in the presence of the CDC7 inhibitors LY3177833 or TAK-931 at the indicated concentration for 4 days. SA-β-Gal staining revealed that CDC7 inhibitors (LY3177833 or TAK-931) selectively induced senescence in *TP53* mutant liver cancer cells (blue) and not in *TP53* wild-type liver cancer cells (red). **g,** *TP53* mutant liver cancer cell lines (Hep3B and Huh7) and *TP53* wild-type liver cancer cell lines (SK-Hep1 and Huh6) were stably transduced with control pLKO vector or with two independent shRNAs targeting *CDC7* (shCDC7#1, shCDC7#2) and the efficiency of CDC7 knockdown in liver cancer cell lines was evaluated by western blot. **h,** Colony formation assays of *TP53* mutant (blue) and *TP53* wild-type liver cancer cell lines (red) with and without CDC7 knockdown were performed. Cells were fixed, stained, and photographed after 10 days of culture. **i,** CDC7 knockdown induced senescence in *TP53* mutant Hep3B and Huh7 cells, but not in *TP53* wild-type SK-Hep1 and Huh6 cells. Senescence was detected by SA-β-Gal staining. For gel source images, see Supplementary Figure 1. Data in **a-i** are representative of three independent biological experiments.

Europe PMC Funders Author Manuscripts

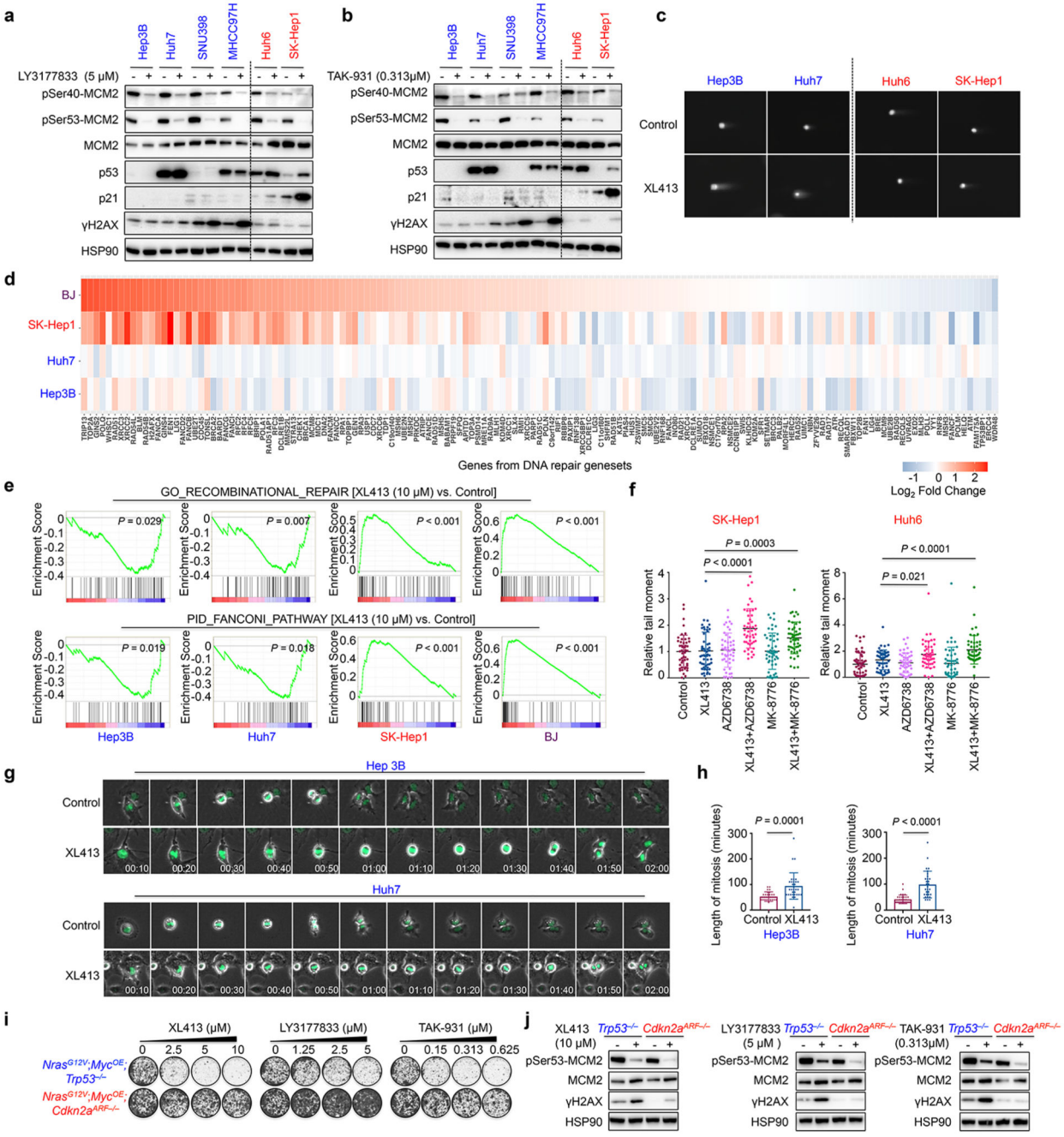

Extended Data Figure 4. CDC7 inhibition leads to DNA damage accumulation specifically in *TP53* mutant liver cancer cells.

a, b, Western blot analysis of liver cancer cell lines treated with CDC7 inhibitors (LY3177833 or TAK-931) for 7 days. CDC7 inhibition induces the expression of the DNA damage marker γH2AX in *TP53* mutant liver cancer cells while lower γH2AX together with functional upregulation of p53 and $p21^{cip1}$ were observed in *TP53* wild-type liver cancer cell lines post-XL413 treatment. **c,** Representative neutral comet assay images of *TP53* mutant (Hep3B and Huh7) and *TP53* wild-type (SK-Hep1 and Huh6) liver cancer cell

Europe PMC Funders Author Manuscripts

lines treated with XL413 for 7 days. **d,** Heatmap displays $\log_2$ fold gene expression changes in *TP53* wild type (BJ and SK-Hep1) and *TP53* mutated (Huh7 and Hep3B) cells upon XL413 treatment (10 μM, 4 days). **e,** Gene set enrichment analysis (GSEA) was performed in RNA sequencing data from Hep3B, Huh7, SK-Hep1 and BJ cells treated with 10 μM XL413 for 4 days and identified DNA repair signatures (Recombinational Repair and Fanconi Anemia Pathway) to be significantly different in *TP53* mutant and *TP53* wild-type cells (See methods for more detailed information). **f,** Neutral comet assays were performed on SK-Hep1 and Huh6 cells treated with 20 μM XL413 combined with AZD6738 (ATR inhibitor, 2.5 uM) or MK-8776 (CHK1 inhibitor, 2.5 uM) for 3 days. The value of tail moments in each treatment group were normalized based on the mean value of the control cells (n=50 per cell line/condition, graphs represent mean ± s.d., analysed with unpaired two-sided Student *t*-test. **g, h,** H2B-GFP Hep3B and Huh7 cells were cultured in absence or presence of XL413 (10 μM) and time-lapse microscopy was performed over 96 h to measure the length of mitosis (Graphs represent mean ± s.d., n=30 per cell line/condition, analysed with unpaired two-sided *t*-test). **i,** Mouse liver cancer cell lines with different genetic background ($Nras^{G12V}$;Myc^{OE};$Trp53^{-/-}$ and $Nras^{G12V}$;Myc^{OE};$Cdkn2a^{ARF-/-}$) were exposed to the indicated concentrations of CDC7 inhibitors (XL413, LY3177833 or TAK-931) for 7 days in colony formation assays. **j,** Western blot analysis of mouse liver cancer cell lines treated with XL413, LY3177833 or TAK-931 for 7 days. For gel source images, see Supplementary Figure 1. Data in **a-c, f, g, h** are representative of two independent biological experiments. Data in **i, j** are representative of three independent biological experiments.

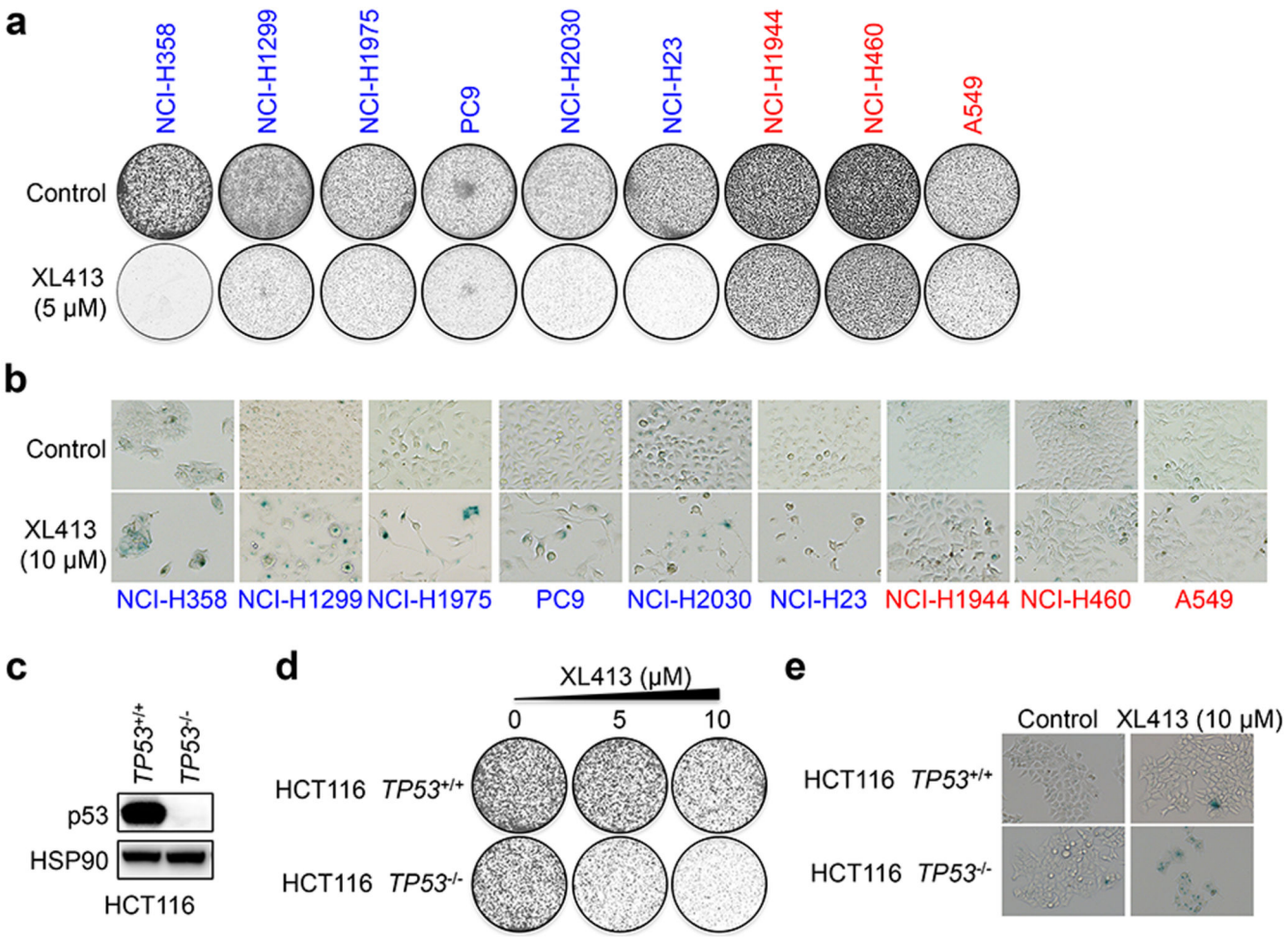

Extended Data Figure 5. CDC7 inhibition induces senescence selectively in *TP53* mutant cancer cells.

a, *TP53* mutant lung cancer cell lines (blue) and *TP53* wild-type lung cancer cell lines (red) were seeded at low confluence and grown in the absence or presence of XL413 at the indicated concentration for 10-14 days in colony formation assays. **b,** Lung cancer cells were exposed to 10 μM XL413 for 4 days, which induces senescence selectively in *TP53* mutant cells as detected by SA-β-gal staining. **c**, p53 expression was assessed in isogenic *TP53*$^{-/-}$ and *TP53*$^{+/+}$ HCT116 colon cancer cell lines by western blot. **d,** HCT116 *TP53*$^{+/+}$ and HCT116 *TP53*$^{-/-}$ cells were seeded at low confluence and grown in the absence or presence of XL413 at the indicated concentration for 7 days in a colony formation assay to assess their proliferation capacity. **e,** HCT116 *TP53*$^{+/+}$ and HCT116 *TP53*$^{-/-}$ cells were cultured in the presence of 10 μM XL413 for 4 days, and senescence was selectively induced in *TP53*$^{-/-}$ HCT116, as detected by SA-β-Gal staining. For gel source images, see Supplementary Figure 1. Data in **a-e** are representative of two independent biological experiments.

Europe PMC Funders Author Manuscripts

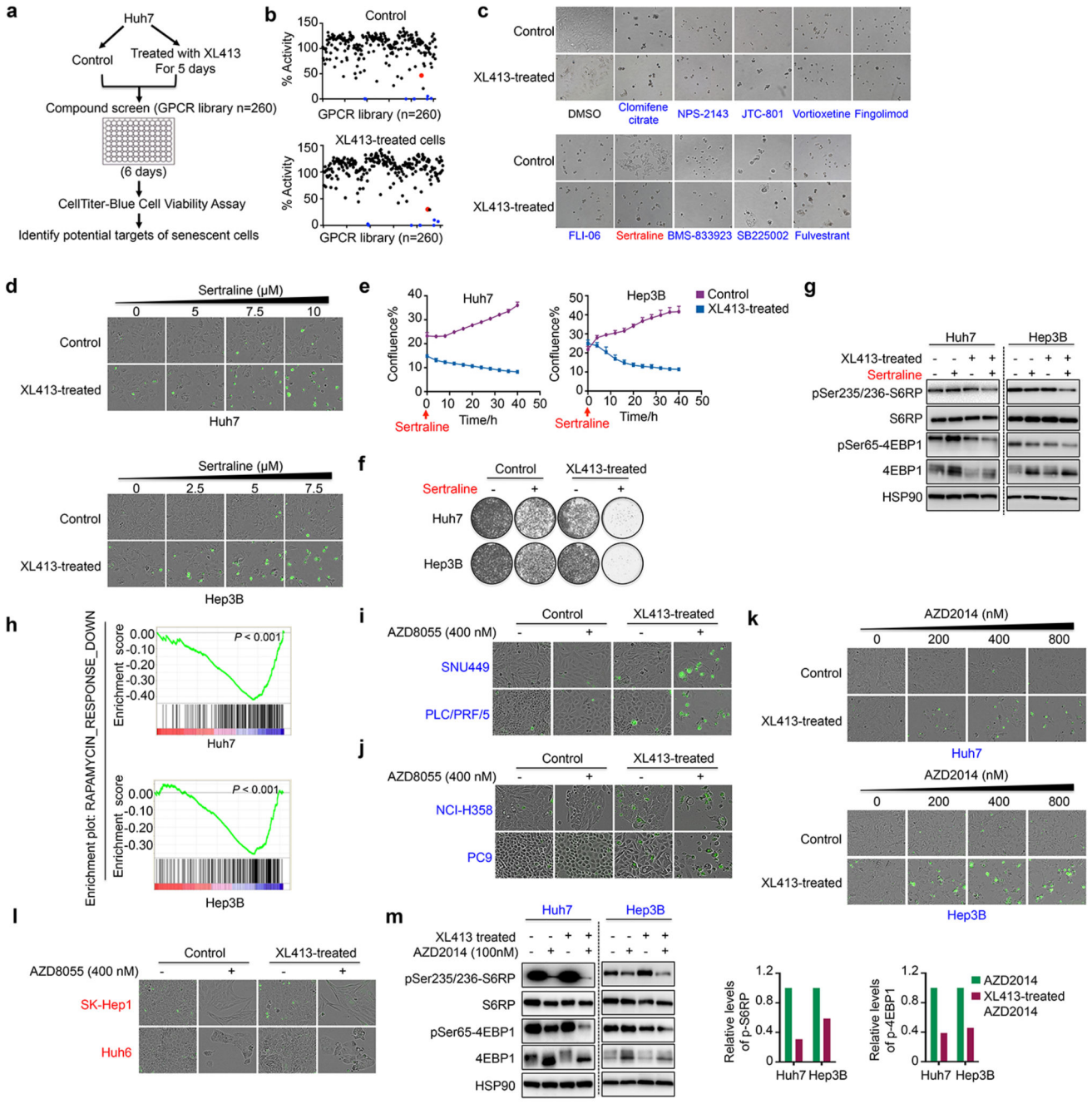

Extended Data Figure 6. Sertraline selectively induces apoptosis in XL413-induced senescent cells through suppression of mTOR signalling.

a, Schematic outline of the GPCR compound screen. Huh7 cells were treated with 10 μM XL413 for 5 days prior to seeding in 96-well plates. All compounds were tested at 4 different concentrations for 6 days and cell viability was measured using CellTiter-Blue assay. **b, c,** Graph depicting the effects of compounds on cell viability. Each point represents a single compound, with % activity calculated by dividing the cell viability score in the presence of 5 μM of that compound by the mean viability of the negative control. Blue dots

Europe PMC Funders Author Manuscripts

indicate compounds inducing cell death in both control and XL413-induced senescent cells. Sertraline (red dot) induced selective cell death in XL413-induced senescent cells. Representative images of the effects of different compounds on XL413-treated and untreated cells were shown. **d,** Control cells and XL413-induced senescent cells were sequentially cultured with increasing concentrations of sertraline for 48 h and apoptotic cells were visualized by caspase-3/7 apoptosis assay. **e,** Control and XL413-treated cells were sequentially exposed to 10 μM sertraline and growth curves were measured by Incucyte live cell assay (Graphs represent mean ± s.d. from three technical replicates). **f,** Control and XL413-treated cells were sequentially treated with vehicle or 10 μM sertraline for 96 h in colony formation assay. **g,** Control and XL413-treated Huh7 and Hep3B cells were treated with sertraline (10 μM) for 24 h and western blot analyses of the indicated mTOR signalling pathway proteins were performed. **h,** Hep3B and Huh7 cells were treated with 10 μM XL413 for 10 days prior to sequential sertraline treatment (10 μM, 24 h) and RNA sequencing was performed. GSEA indicates that the gene set related to downregulation of mTOR signalling was negatively enriched in liver cancer cells sequentially treated with XL413 and sertraline (See methods for more detailed information). **i-j,** *TP53* mutant liver cancer cell lines (SNU449 and PLC/PRF/5) and lung cancer cell lines (NCI-H358 and PC9) were treated with 10 μM XL413 or vehicle for 5-7 days and sequentially exposed to increasing concentrations of AZD8055. Apoptotic cells were visualized by caspase-3/7 apoptosis assay 96 h post-AZD8055 treatment. **k,** *TP53* mutant Hep3B and Huh7 cells were treated with 10 μM XL413 or vehicle for 7-10 days. Control cells and XL413-induced senescent cells were plated and exposed to increasing concentrations of the mTORC1/2 inhibitor AZD2014 prior to caspase-3/7 apoptosis assay at 96 h. **l,** *TP53* wild-type liver cancer cell lines (SK-Hep1 and Huh6) were treated with 10 μM XL413 or vehicle for 5-7 days prior to exposure to increasing concentrations of AZD8055. Apoptotic cells were visualized by caspase-3/7 apoptosis assay 96 h post-AZD8055 treatment. **m,** Control cells and XL413-induced senescent cells were treated with AZD2014 for 48 h. Western blot analysis was performed with the indicated antibodies (left panel) and the levels of p-S6RP and p-4EBP1 was normalized to total-S6RP and total-4EBP1, respectively (right panel), showing that AZD2014 treatment leads to strong mTOR signalling inhibition in XL413-induced senescent cells. For gel source images, see Supplementary Figure 1. Data in **a-f** are representative of three independent biological experiments. Data in **h-m** are representative of two independent biological experiments.

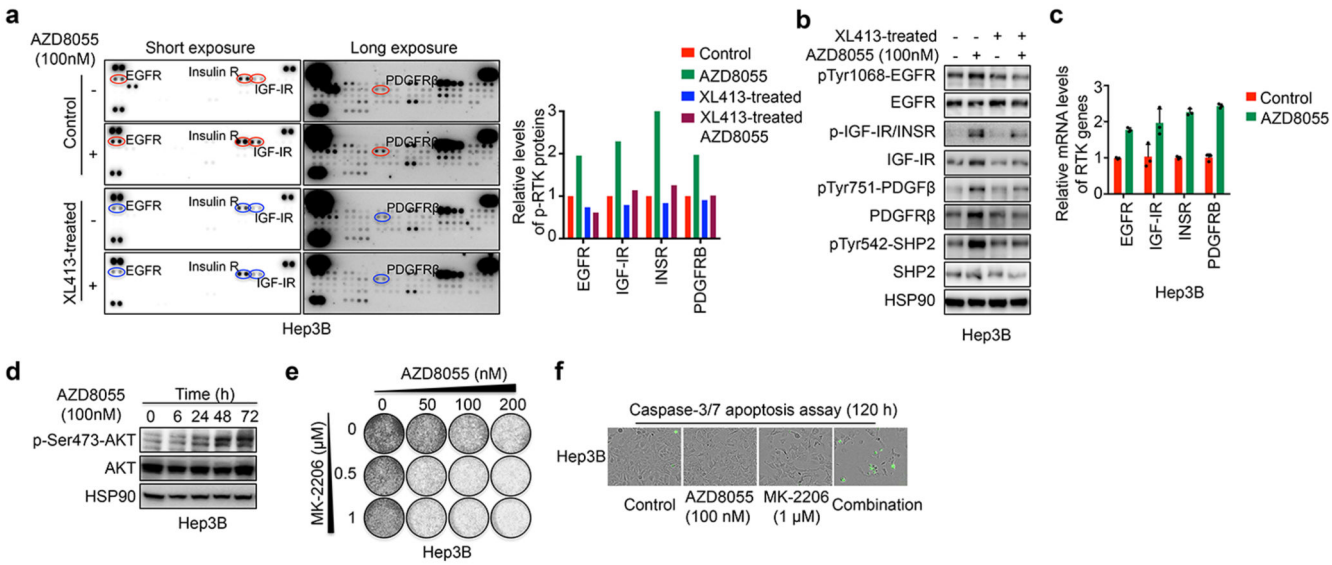

Extended Data Figure 7. The Receptor Tyrosine Kinase feedback activation induced post-AZD8055 treatment is disrupted in XL413-induced senescent cells.

a, Control cells and XL413-treated Hep3B cells were treated with AZD8055 for 48 h and extracted proteins were analysed using a Human Phospho-Receptor Tyrosine Kinase Array Kit (left panel). The levels of p-RTK proteins were normalized to positive controls (right panel). **b,** Activation of Receptor Tyrosine Kinases (RTKs) identified by RTK arrays and phosphorylation of SHP2 were validated by western blot analyses. **c,** Hep3B cells were treated with AZD8055 for 48 h prior to mRNA extraction and quantification of the indicated Receptor Tyrosine Kinase genes were performed by qRT-PCR analysis (Graph represents mean ± s.d. from three technical replicates). **d,** Hep3B cells were treated with AZD8055, and cell lysates were collected at the indicated time points to perform western blot analyses with the indicated antibodies. **e,** Hep3B cells were exposed to increasing concentrations of the AKT inhibitor (MK-2206) in combination with AZD8055 and long-term colony formation assays were performed, revealing the synergistic effects of these compounds on cell viability. **f,** Hep3B cells were treated with AZD8055, MK-2206 or the combined compounds at the indicated concentrations for 5 days and apoptotic cells were visualized by caspase-3/7 apoptosis assay. For gel source images, see Supplementary Figure 1. All experiments shown, except for the RTK array analyses, are representative of two independent biological experiments.

Europe PMC Funders Author Manuscripts

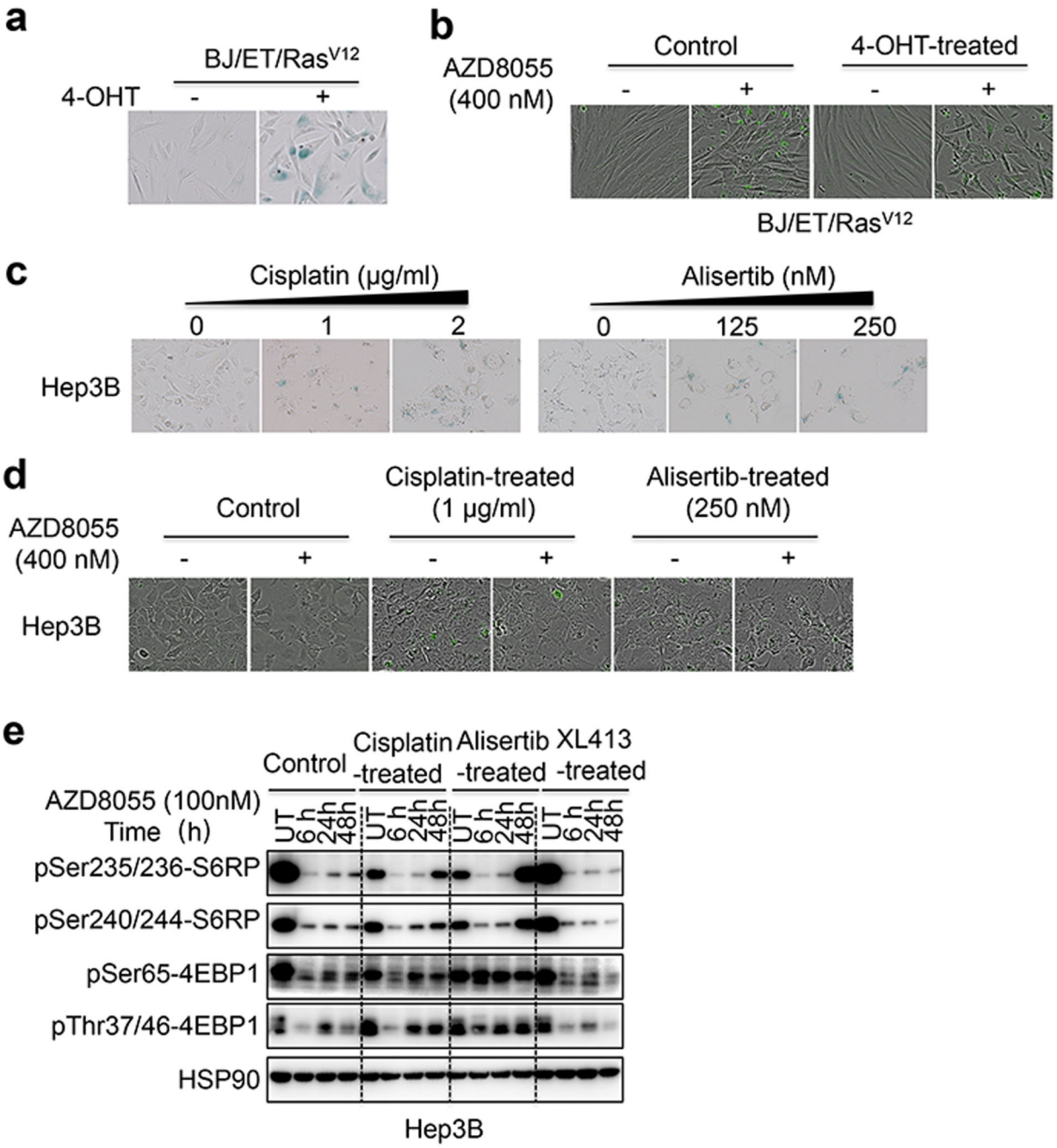

Extended Data Figure 8. AZD8055 does not induce apoptosis in Cisplatin or Alisertib-induced senescent cells

a, BJ/ET/Ras^{V12} cells were treated with 100 nm 4-OHT for 21 days to induce senescence, as detected by SA-β-gal staining. **b,** Control or senescent BJ/ET/Ras^{V12} cells were treated with either vehicle or 400 nM AZD8055 for 96 hours and apoptotic cells were visualized by caspase-3/7 apoptosis assay. **c,** Hep3B cells were cultured in the presence of Cisplatin or Alisertib (Aurora-A kinase inhibitor) for 4 days at the indicated concentrations and senescence induction was detected by SA-β-gal staining. **d,** Hep3B cells were treated with

Europe PMC Funders Author Manuscripts

Cisplatin (1 μg/ml) or Alisertib (250 nM) for 4 days and subsequently exposed to vehicle or 400 nM AZD8055 for 96 hours. Apoptotic cells were visualized by caspase-3/7 apoptosis assay. **e,** Control cells, Cisplatin, Alisertib or XL413-induced senescent cells were treated with AZD8055, and cell lysates were collected at the indicated time points. Western blot analyses were performed with the indicated antibodies revealing that mTOR signalling feedback loop is functional in Cisplatin and Alisertib-induced senescent cells while it is efficiently inhibited in XL413-induced senescent cells. For gel source images, see Supplementary Figure 1. Data in **a-e** are representative of two independent biological experiments.

Europe PMC Funders Author Manuscripts

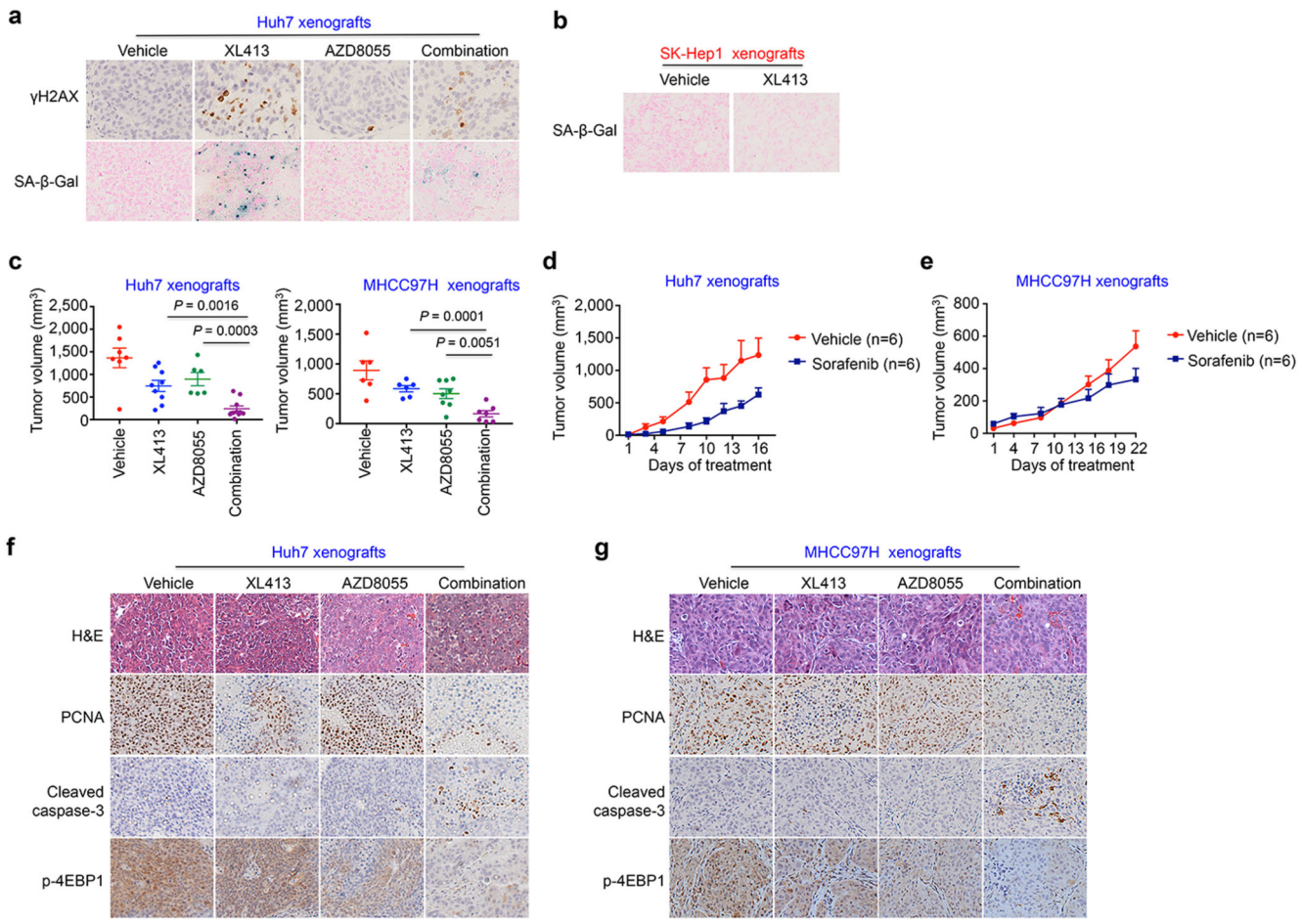

Extended Data Figure 9. Pro-senescence treatment combined with mTOR inhibitor suppresses tumour growth in liver cancer xenografts.

a, Representative images of γH2AX and SA-β-Gal staining performed on formalin-fixed, paraffin-embedded or frozen sections from subcutaneous Huh7 xenografts treated with vehicle, XL413, AZD8055 or combination for 12 days. **b,** Representative images of SA-β-Gal staining performed on frozen sections from subcutaneous SK-Hep1 xenografts treated either with vehicle or XL413 for 21 days. **c,** Tumour volume measurements in vehicle, XL413, AZD8055 or combination-treated mice bearing Huh7 and MHCC97H xenografts at endpoint (12 days and 22 days, respectively, for sample size see Figure 4a). One mouse in the vehicle group and one mouse in the XL413 group were excluded in the analysis, since the maximum permitted tumour volumes (2,000 mm^3) were reached prior to trial endpoint. Graph shows mean ± s.e.m., analysed with two-sided unpaired Student *t*-test. **d, e,** Longitudinal tumour volume progression in Huh7 and MHCC97H tumour-bearing mice treated with vehicle or sorafenib for 16 or 22 days, revealing that sorafenib therapy displays limited efficacy in these two different xenograft models. Graph shows mean ± s.e.m. **f, g,** Representative images of H&E, PCNA, cleaved caspase-3 and p-4EBP1 staining performed on formalin-fixed, paraffin-embedded Huh7 and MHCC97H xenografts from mice sacrificed after the last dose of vehicle, XL413, AZD8055 or combination treatment. Data in **a, b, f, g** are representative of three independent biological experiments.

Europe PMC Funders Author Manuscripts

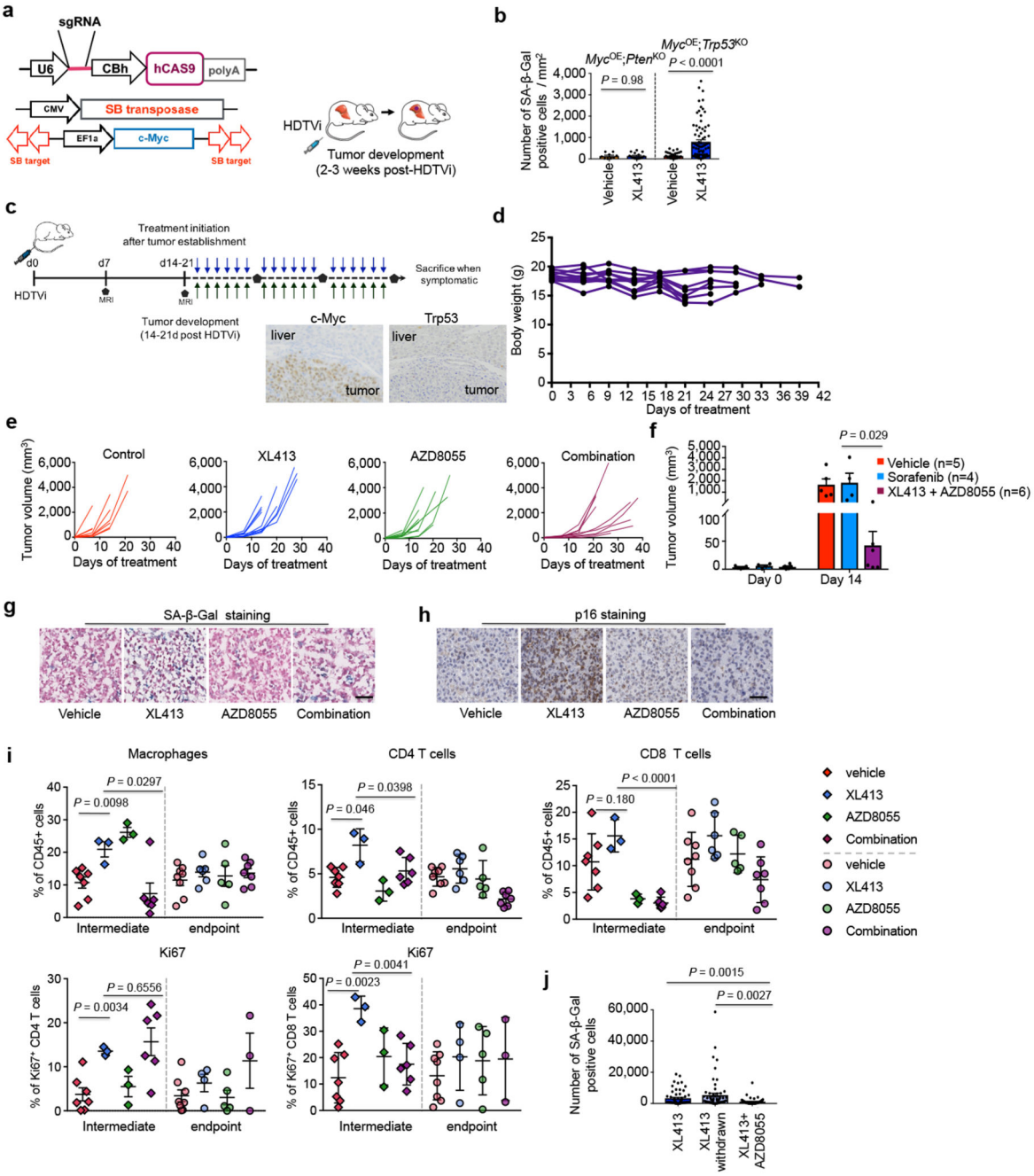

Extended Data Figure 10. Pro-senescence treatment combined with mTOR inhibitor suppresses tumour growth in p53-deficient, immunocompetent somatic murine models of HCC

a, Schematic representation of hydrodynamic tail vein gene delivery of the c-Myc proto-oncogene transposon system and a CRISPR-Cas9 vector targeting either *Trp53* or *Pten* tumour suppressor, used to induce HCC 2-3 weeks post-HDTV injection (HDTVi). **b,** Quantification of SA-β-Gal staining performed on frozen sections from *Myc*^{OE};*Pten*^{KO} or *Myc*^{OE};*Trp53*^{KO} HCC 14 days post treatment with vehicle or XL413 monotherapy (*Myc*^{OE};*Trp53*^{KO} also showed in Fig. 4f). For *Myc*^{OE};*Pten*^{KO} analyses: vehicle, n=9

Europe PMC Funders Author Manuscripts

biologically independent nodules out of 3 mice; XL413, n=16 biologically independent nodules out of 3 mice. For *Myc*^{OE};*Trp53*^{KO}, vehicle, n=41 biologically independent nodules out of 7 mice; XL413, n=81 biologically independent nodules out of 11 mice. Graph shows the mean ± s.e.m. of the number of SA-β-Gal positive cells per tumour nodule/mm^2. Statistics were calculated by two-sided unpaired Student *t*-test. **c,** Trial design to evaluate the efficacy of the pro-senescence treatment combined with mTOR inhibitor in *Myc*^{OE};*Trp53*^{KO} HCC-bearing mice: Animals were monitored by weekly MRI post-HDTVi and enrolled into vehicle, XL413 (100mg/kg, daily gavage), AZD8055 (20mg/kg, daily gavage) or XL413+AZD8055 combination treatment groups at first signs of tumour development by MRI. Drugs were administered 6 days / week, and mice were sacrificed when symptomatic. Immunohistochemical (IHC) analyses confirmed Myc expression and p53 knockout in endpoint *Myc*^{OE};*Trp53*^{KO} HCC. **d,** Longitudinal individual body weight curves from *Myc*^{OE};*Trp53*^{KO} tumour-bearing mice treated with the combination of XL413+AZD8055 therapies. **e,** Individual tumour growth curves from mice treated with vehicle, XL413, AZD8055 or combination treatment were calculated based on MRI images from *Myc*^{OE};*Trp53*^{KO} tumour-bearing mice. **f,** *Myc*^{OE};*Trp53*^{KO} tumour volumes from HCC-bearing mice treated with vehicle (n=5, as shown in Fig. 4c), Sorafenib (n=4) or XL413 + AZD8055 (n=6) at day 0 and day 14. Graphs show mean ± s.e.m. analysed with two-sided unpaired Student *t*-test. **g, h,** Representative images of SA-β-Gal (**g**) and p16 (**h**) staining performed on frozen and paraffin-embedded sections, respectively, from *Myc*^{OE};*Trp53*^{KO} tumour-bearing mice treated with the indicated drugs and sacrificed at the intermediate timepoint (14-16 days in time-matched treated cohorts. Quantification are shown in Fig. 4f, g). Scale bar, 50 μm. **i,** *Myc*^{OE};*Trp53*^{KO} tumour-bearing mice treated with vehicle, XL413, AZD8055 or combination were sacrificed at the indicated time point post-treatment. Tumours were dissociated as single cell suspension and flow cytometry analyses were performed to determine the content of tumour-associated macrophages (CD45$^+$ CD11b$^+$Ly6C$^-$Ly6G$^-$), CD8 T cells (CD45$^+$ CD3$^+$CD19$^-$ NK1.1$^-$CD8$^+$) and CD4 T cells (CD45$^+$ CD3$^+$ CD19$^-$ NK1.1$^-$CD4$^+$) relative to total CD45$^+$ leucocytes and cell proliferation (Ki67$^+$) was determined within CD8 T cells and CD4 T cell populations. Graphs show mean ± s.e.m., analysed with two-sided unpaired Student *t*-test (for sample size, see methods). **j,** *Myc*^{OE};*Trp53*^{KO} HCC-bearing mice were treated with XL413 (n=20) or XL413+AZD8055 combination (n=8) for 14 days. Among the XL413-treated mice, a subset (n=10) was sacrificed directly 14 days post treatment, concomitantly to the combination-treated group. The rest of the XL413-treated mice (n=10) underwent XL413-drug withdrawal for 4 days. The absolute number of senescent cells per tumour nodule were visualized by SA-β-Gal staining performed on frozen sections and quantified for each treatment group (XL413 n=60 biologically independent nodules out of 10 mice; XL413 withdrawn n=63 biologically independent nodules out of 10 mice; XL413+AZD8055 n=57 biologically independent nodules out of 7 mice). Graphs show mean ± s.e.m. analysed with two-sided unpaired Student *t*-test. Data in **c** are representative of three independent biological experiments.

Supplementary Material

Refer to Web version on PubMed Central for supplementary material.

Acknowledgements

We thank Lars Zender, Ron Smits, Xiaohang Qiao and Li Li for the kind gift of cell lines. This work was funded by grants from the European Research Council (ERC 787925 to R.B.), the Dutch Cancer Society (KWF 12049/2018-2 to L.A, 6702/2014 to B.B and H.t.R) through the Oncode Institute and the Center for Cancer Genomics (CGC.nl), the National Basic Research Program of China (973 Program: 2015CB553905), the National Key Sci-Tech Special Projects of Infectious Diseases of China (2018ZX10732202-002-003), the National Natural Science Foundation of China (81920108025, 81421001, 81672933 and 81874229), Shanghai Municipal Education Commission-Gaofeng Clinical Medicine Grant Support (20181703), Shanghai Municipal Commission of Health and Family Planning (2017YQ064 and 2018YQ20), and Shanghai Rising-Star Program (18QA1403900). We thank the facilities of Netherlands Cancer Institute: Animal Laboratory, Mouse Clinic Imaging Unit, Experimental Animal Pathology, Flow Cytometry, Sequencing, and BioImaging.

References

1. Bray F, et al. Global cancer statistics 2018: GLOBOCAN estimates of incidence and mortality worldwide for 36 cancers in 185 countries. CA Cancer J Clin. 2018; 68:394–424. [PubMed: 30207593]
2. Llovet JM, et al. Hepatocellular carcinoma. Nat Rev Dis Primers. 2016; 2
3. Llovet JM, et al. Sorafenib in advanced hepatocellular carcinoma. N Engl J Med. 2008; 359:378–390. [PubMed: 18650514]
4. Wang L, et al. High-Throughput Functional Genetic and Compound Screens Identify Targets for Senescence Induction in Cancer. Cell Rep. 2017; 21:773–783. [PubMed: 29045843]
5. Sieben CJ, Sturmlechner I, van de Sluis B, van Deursen JM. Two-Step Senescence-Focused Cancer Therapies. Trends Cell Biol. 2018; 28:723–737. [PubMed: 29776716]
6. Rodrik-Outmezguine VS, et al. mTOR kinase inhibition causes feedback-dependent biphasic regulation of AKT signaling. Cancer Discov. 2011; 1:248–259. [PubMed: 22140653]
7. Zucman-Rossi J, Villanueva A, Nault JC, Llovet JM. Genetic Landscape and Biomarkers of Hepatocellular Carcinoma. Gastroenterology. 2015; 149:1226–1239 e1224. [PubMed: 26099527]
8. Chang J, et al. Clearance of senescent cells by ABT263 rejuvenates aged hematopoietic stem cells in mice. Nat Med. 2016; 22:78–83. [PubMed: 26657143]
9. Ogrodnik M, et al. Cellular senescence drives age-dependent hepatic steatosis. Nat Commun. 2017; 8
10. Wang C, et al. A CRISPR screen identifies CDK7 as a therapeutic target in hepatocellular carcinoma. Cell Res. 2018; 28:690–692. [PubMed: 29507396]
11. Koltun ES, et al. Discovery of XL413, a potent and selective CDC7 inhibitor. Bioorg Med Chem Lett. 2012; 22:3727–3731. [PubMed: 22560567]
12. Montagnoli A, Moll J, Colotta F. Targeting cell division cycle 7 kinase: a new approach for cancer therapy. Clin Cancer Res. 2010; 16:4503–4508. [PubMed: 20647475]
13. Cancer Genome Atlas Research Network. Comprehensive and Integrative Genomic Characterization of Hepatocellular Carcinoma. Cell. 2017; 169:1327–1341 e1323. [PubMed: 28622513]
14. Fridman AL, Tainsky MA. Critical pathways in cellular senescence and immortalization revealed by gene expression profiling. Oncogene. 2008; 27:5975–5987. [PubMed: 18711403]
15. Faget DV, Ren Q, Stewart SA. Unmasking senescence: context-dependent effects of SASP in cancer. Nat Rev Cancer. 2019; 19:439–453. [PubMed: 31235879]
16. Dauch D, et al. A MYC-aurora kinase A protein complex represents an actionable drug target in p53-altered liver cancer. Nat Med. 2016; 22:744–753. [PubMed: 27213815]
17. Eggert T, et al. Distinct Functions of Senescence-Associated Immune Responses in Liver Tumor Surveillance and Tumor Progression. Cancer Cell. 2016; 30:533–547. [PubMed: 27728804]
18. Lin CJ, Robert F, Sukarieh R, Michnick S, Pelletier J. The antidepressant sertraline inhibits translation initiation by curtailing mammalian target of rapamycin signaling. Cancer Res. 2010; 70:3199–3208. [PubMed: 20354178]

19. Keng VW, et al. A conditional transposon-based insertional mutagenesis screen for genes associated with mouse hepatocellular carcinoma. Nat Biotechnol. 2009; 27:264–274. [PubMed: 19234449]

20. Milanovic M, et al. Senescence-associated reprogramming promotes cancer stemness. Nature. 2018; 553:96–100. [PubMed: 29258294]

21. Georgilis A, et al. PTBP1-Mediated Alternative Splicing Regulates the Inflammatory Secretome and the Pro-tumorigenic Effects of Senescent Cells. Cancer Cell. 2018; 34:85–102 e109. [PubMed: 29990503]

22. Flynn MJ, Sayed AA, Sharma R, Siddique A, Pinato DJ. Challenges and Opportunities in the Clinical Development of Immune Checkpoint Inhibitors for Hepatocellular Carcinoma. Hepatology. 2019; 69:2258–2270. [PubMed: 30382576]

23. Garcia Fortanet J, et al. Allosteric Inhibition of SHP2: Identification of a Potent, Selective, and Orally Efficacious Phosphatase Inhibitor. J Med Chem. 2016; 59:7773–7782. [PubMed: 27347692]

24. Evers B, et al. CRISPR knockout screening outperforms shRNA and CRISPRi in identifying essential genes. Nat Biotechnol. 2016; 34:631–633. [PubMed: 27111720]

25. Koelzer VH, et al. Digital image analysis improves precision of PD-L1 scoring in cutaneous melanoma. Histopathology. 2018; 73:397–406. [PubMed: 29660160]

26. Subramanian A, et al. Gene set enrichment analysis: a knowledge-based approach for interpreting genome-wide expression profiles. Proc Natl Acad Sci U S A. 2005; 102:15545–15550. [PubMed: 16199517]

27. Peng T, Golub TR, Sabatini DM. The immunosuppressant rapamycin mimics a starvation-like signal distinct from amino acid and glucose deprivation. Mol Cell Biol. 2002; 22

28. Olive PL, Banath JP. The comet assay: a method to measure DNA damage in individual cells. Nat Protoc. 2006; 1:23–29. [PubMed: 17406208]

Europe PMC Funders Author Manuscripts

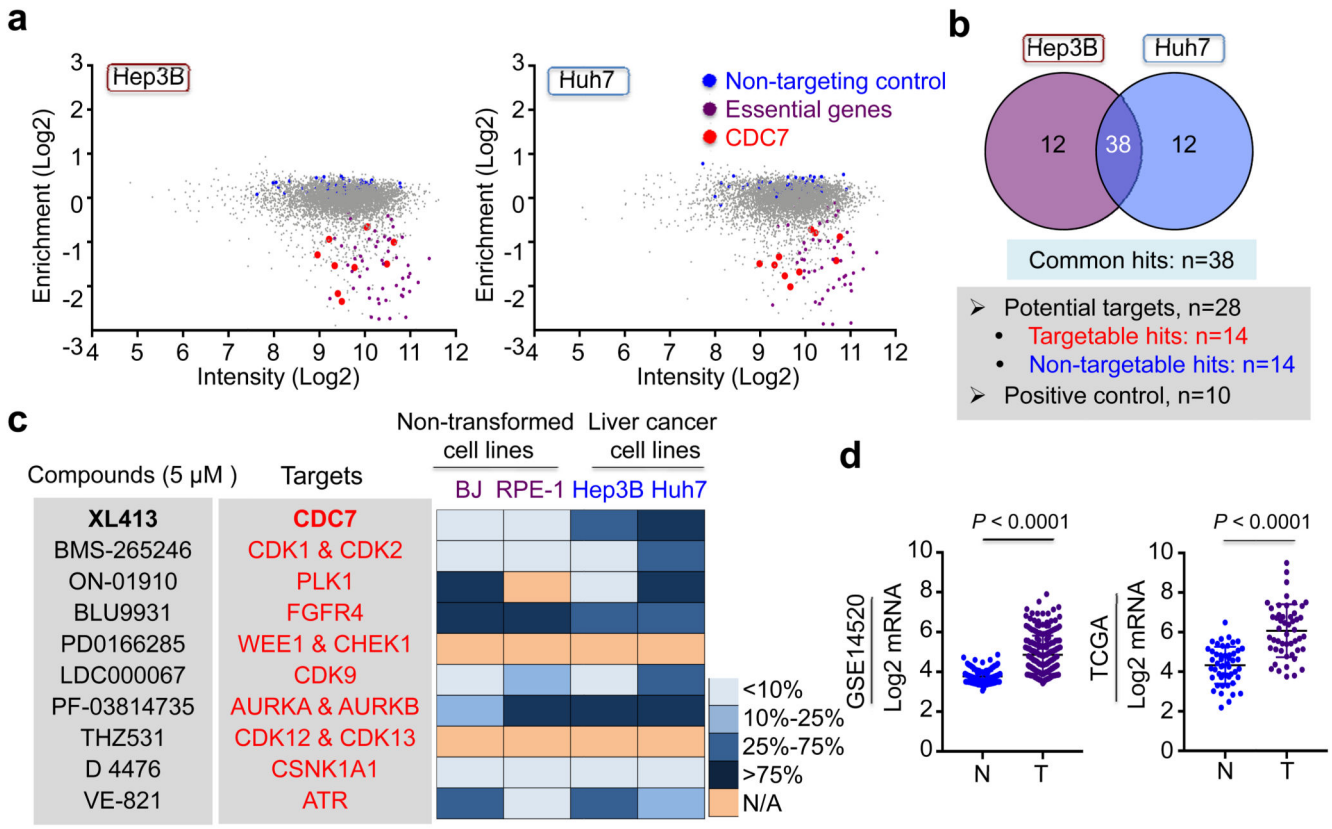

Figure 1. A two-step screen identifies CDC7 as a target for senescence-inducing strategy in liver cancer.

a, Hep3B and Huh7 cells were transduced with a lentiviral kinome gRNA library and three independent replicates were cultured for 14 days (T14). gRNA barcodes from T0 and T14 samples were recovered by PCR and analysed by next generation sequencing. The y axis shows log2-fold change in abundance (ratio of gRNA frequency in T14 sample to that in T0 sample). The x axis depicts the average read-count in the T0 sample. **b,** 38 common hits (among top 50 most strongly depleted hits in each cell line) were identified by CRISPR screen in Hep3B and Huh7 cells. **c**, Heatmap indicates the effects of compounds (ten compounds targeting 14 hits identified by CRISPR screen, 5 μM for 4 day-treatments) on inducing senescence-associated β-galactosidase (SA-β-Gal) activity in non-transformed cell lines (BJ and RPE-1) and liver cancer cell lines (Hep3B and Huh7). **d,** CDC7 mRNA expression in paired tumour and non-tumour tissues from GSE14520 cohort (n=213) and TCGA database (n=50). Paired two-sided *t*-test. Data in graphs are mean ± s.d. Data in **a-c** are representative of three independent biological experiments.

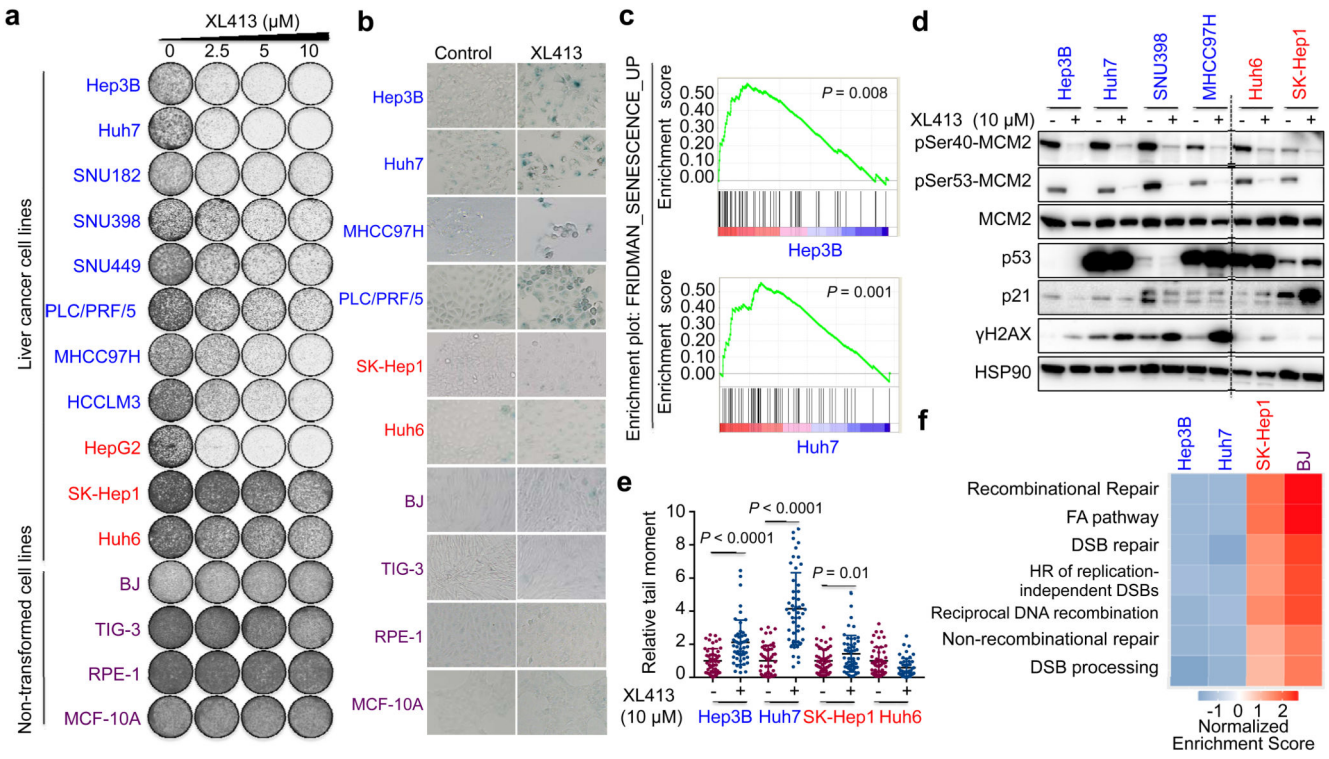

Figure 2. CDC7 inhibition selectively induces senescence in *TP53* mutant liver cancer cells.

a, Long-term colony formation assay was performed over 10-14 days on *TP53* mutant liver cancer cell lines (blue), *TP53* wild-type liver cancer cell lines (red), and non-transformed cell lines (purple) cultured with the indicated concentrations of XL413. **b,** Liver cancer cells and non-transformed cell lines were cultured in the presence of 10 μM XL413 for 4 days and induction of senescence was assessed by staining for SA-β-Gal activity. **c,** GSEA (gene set enrichment analysis) of senescence signature (FRIDMAN_SENESCENCE_UP) in sequence data from Hep3B and Huh7 cells treated with 10 μM XL413 for 4 days (See methods for more detailed information). **d,** Proteins were extracted from *TP53* mutant and wild-type liver cancer cell lines treated with XL413 (10 μM) for 7 days and analysed by western blotting. **e,** Neutral comet assays were performed on Hep3B, Huh7, SK-Hep1 and Huh6 cells cultured with 10 μM XL413 for 7 days. The value of tail moments in each treatment group were normalized based on the mean value of the control cells. (n=50 per cell line/condition, data in graphs are mean ± s.d. and analysed by unpaired two-sided *t*-test). **f,** GSEA in *TP53* mutant (Hep3B and Huh7) and *TP53* wild-type (SK-Hep1 and BJ) cells treated with 10 μM XL413 for 4 days (FA=Fanconi Anemia, DSB=double strand break, HR=homologous recombination). For gel source images, see Supplementary Figure 1. Data in **a, b** are representative of three independent biological experiments. Data in **d, e** are representative of two independent biological experiments.

Europe PMC Funders Author Manuscripts

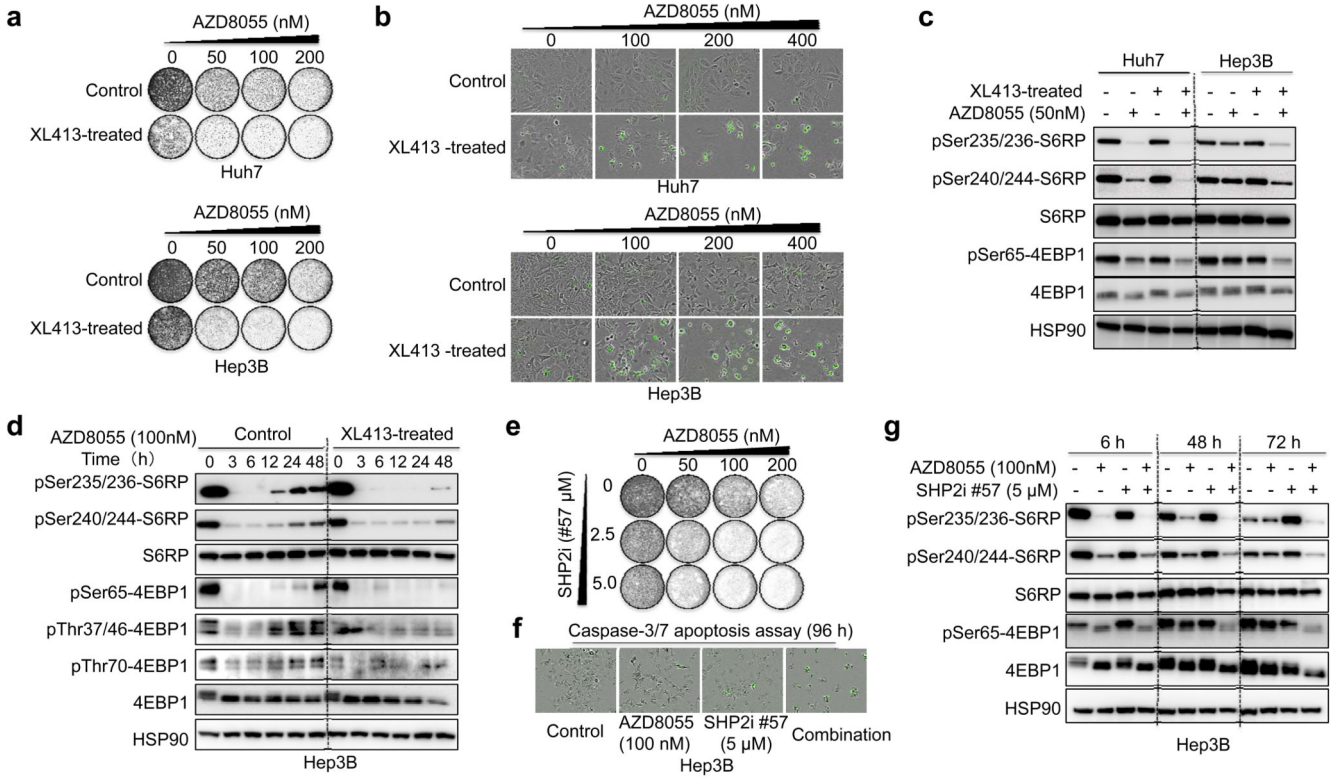

Figure 3. AZD8055 selectively triggers apoptosis in XL413-induced senescent cells.

a, Hep3B and Huh7 cells were treated with 10 μM XL413 or vehicle for 10 days prior to sequential exposure to increasing concentrations of AZD8055 for 5-7 days in colony formation assays. **b,** Apoptotic cells were determined by caspase-3/7 apoptosis assay 96 h after AZD8055 treatment. **c,** Control cells and XL413-induced senescent cells were treated with AZD8055 for 48 h prior to western blot analyses with the indicated antibodies. **d,** Control cells and XL413-induced senescent cells were treated with AZD8055, and cell lysates were collected at the indicated time points prior to western blot analyses with the indicated antibodies. **e, f,** Long-term colony formation and caspase-3/7 apoptosis assays showing the synergistic effect of mTOR and SHP2 inhibitors on Hep3B proliferation. **g,** Hep3B cells were treated with AZD8055, SHP2 inhibitor or the combination of both drugs at the indicated time points prior to western blot analysis with the indicated antibodies. For gel source images, see Supplementary Figure 1. Data in **a-f** are representative of three independent biological experiments. Data in **g** are representative of two independent biological experiments.

Europe PMC Funders Author Manuscripts

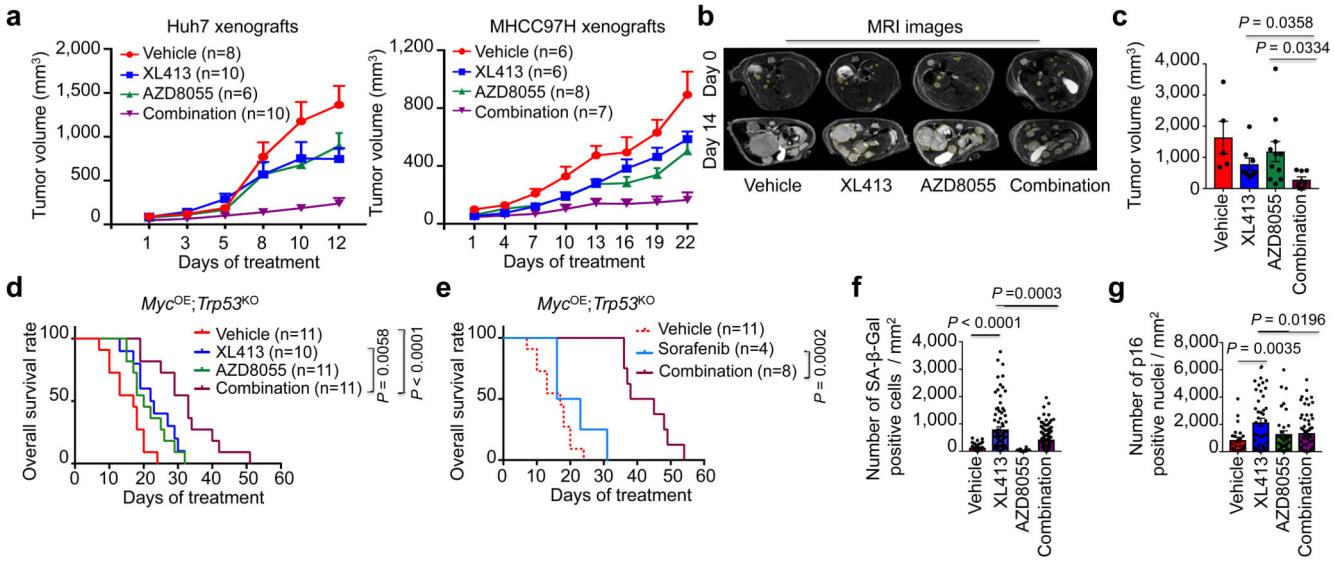

Figure 4. CDC7 inhibition induces senescence *in vivo* and suppresses tumour growth when combined with mTOR inhibition in multiple liver cancer models.

a, Huh7 and MHCC97H cells were grown as tumour xenografts in BALB/c nude mice. Longitudinal tumour volume progression in Huh7 and MHCC97H tumour-bearing mice treated with vehicle, XL413, AZD8055 or combined therapies for 12 or 22 days, respectively. Graph shows mean ± s.e.m. **b-g,** Analyses of combination therapy response in the *Myc*^{OE};*Trp53*^{KO} HCC somatic murine model. **b,** Representative MRI images out of 9 independent experimental cohorts, of day 0 and day 14 of mice enrolled in vehicle, XL413, AZD8055 or combination treatment. The yellow line indicates the visible tumour area used to calculate the tumour volume. **c,** Tumour volumes were calculated based on MRI images from HCC-bearing mice with matched initial tumour volume. Graph shows mean ± s.e.m. from mice treated with vehicle (n=5), XL413 (n=8), AZD8055 (n=11) or combination (n=8) at the intermediate time point post-treatment initiation (day 14-16 in matched treatment groups, unpaired two-sided *t*-test). **d,** Survival curve generated from *Myc*^{OE};*Trp53*^{KO}-tumour bearing mice treated with vehicle (n=11; median survival 17 days), XL413 (n=10; median survival 22.5 days), AZD8055 (n=11; median survival 20 days) or combination (n=11; median survival 33 days). **e,** Survival curve generated from independent cohorts of *Myc*^{OE};*Trp53*^{KO}-HCC bearing mice treated with sorafenib (n=4; median survival 19.5 days) or combination of XL413 and AZD8055 (n=8; median survival 41.5 days). Vehicle group from Fig. 4d is used as a reference. **d, e,** Statistical significance was calculated using a two-sided Log-rank test. **f, g,** Graphs show mean ± s.e.m. of number of SA-β-Gal^{+} (**f**) or p16^{+} (**g**) cells per tumour nodule/mm^{2} (unpaired two-sided *t*-test. For sample size, see methods).